

DEVELOPMENT OF A THULIUM GERMANATE
THIN DISK LASER PROTOTYPE

by

Daniel Sickinger

Copyright © Daniel Sickinger 2016

A Thesis Submitted to the Faculty of the
COLLEGE OF OPTICAL SCIENCES

In Partial Fulfillment of the Requirements

For the Degree of

MASTER OF SCIENCE

In the Graduate College

THE UNIVERSITY OF ARIZONA

2016

STATEMENT BY AUTHOR

The thesis titled *Development of a Thulium Germanate Thin Disk Laser Prototype* prepared by Daniel Sickinger has been submitted in partial fulfillment of requirements for a master's degree at the University of Arizona and is deposited in the University Library to be made available to borrowers under rules of the Library.

Brief quotations from this thesis are allowable without special permission, provided that an accurate acknowledgement of the source is made. Requests for permission for extended quotation from or reproduction of this manuscript in whole or in part may be granted by the head of the major department or the Dean of the Graduate College when in his or her judgment the proposed use of the material is in the interests of scholarship. In all other instances, however, permission must be obtained from the author.

SIGNED: Daniel Sickinger

APPROVAL BY THESIS DIRECTOR

This thesis has been approved on the date shown below:

<hr/>	<u>Defense Date</u>
Xiushan Zhu	5/9/2016
Associate Research Professor of Optical Sciences	
<hr/>	<u>Defense Date</u>
Nasser N. Peyghambarian	5/9/2016
Professor of Optical Sciences	

Acknowledgements

I would like to take the time to first thank those who have helped me develop and understand lasers fundamentally, most notably, my advisor Xiushan Zhu and Valery Temyanko. Their ability to patiently answer my questions was invaluable to the experience I developed throughout this project.

People to also thank are, Rolland Himmelhuber and Sasaan Showghi for opinions and ideas to point me in the right directions, as well as Todd Horne for the use of the machine shop and tools.

Finally and most importantly, I would like to thank my parents, who I love dearly, for always being there for me under any experience I was facing in life.

Contents

List of Figures.....	v
List of Tables	vii
Abstract.....	viii
Introduction.....	1
1.1 History	2
<i>Rectangular Thin Slab Laser</i>	2
<i>Zig-Zag Thin Slab Laser</i>	3
<i>Thin Disk Laser</i>	4
1.2 Areas of Interest	7
<i>Military Applications</i>	7
<i>Medical Applications</i>	8
<i>Material Processing</i>	8
<i>Laser Sensing and Spectroscopy</i>	9
1.3 Thulium Germanate Thin Disk as Potential.....	9
<i>Thulium Germanate as Gain Medium</i>	10
<i>Thulium Germanate as a Thin Disk Laser</i>	11
1.4 Motivation and Intent	12
Thin Disk Laser Basics	13
2.1 Laser Gain Medium.....	15
<i>Amplifying Atoms</i>	15
<i>Host Material</i>	17
2.2 Laser Oscillator	18
<i>Cavity Configurations</i>	18
<i>Resonator Types</i>	19
2.3 Pumping Configuration	21
<i>Pump Chamber</i>	22

<i>Source Optics</i>	24
Laser Fundamentals and Modelling	25
3.1 Light Interactions	25
<i>Spontaneous Emission</i>	27
<i>Absorption</i>	27
<i>Stimulated Emission</i>	28
3.2 Laser Operation	28
<i>Three Level System</i>	29
<i>Laser Assumptions</i>	31
3.3 Rate Equations.....	33
<i>Population Rate Equations</i>	33
<i>Photon Rate Equations</i>	34
3.4 Gain Threshold.....	35
3.5 Pump Chamber Power Contribution	36
3.6 Resonator Effects	39
<i>Signal Aperture Effect</i>	39
<i>Pump-Signal Coupling Value</i>	40
3.7 CW Power Output Model.....	41
<i>Output Power Equations</i>	41
<i>Yb:YAG Thin Disk Laser Comparison</i>	42
Thin Disk Prototype Design	45
4.1 Design Summary	46
<i>First Order Summary</i>	46
4.2 Component Selection and Manufacture	47
<i>Pump Source</i>	47
<i>Collimation Optics</i>	47
<i>Parabolic Mirror</i>	48
<i>Fold Mirrors</i>	48
<i>Thin Disk</i>	49
<i>Thin Disk Heatsink</i>	50

<i>Resonator Configuration</i>	51
<i>Final System Layout</i>	52
4.3 Alignment and Assembly.....	55
<i>Thin Disk Reference Mirror to Parabolic Mirror</i>	56
<i>Four Fold Mirrors</i>	58
<i>Pump Source and Collimation Optics</i>	60
<i>Thin Disk and Resonator Optics</i>	62
System Performance	63
5.1 Pump Spot Analysis	63
<i>Fiber Source</i>	64
<i>Pump Spot</i>	65
<i>Tm:Germanate Output Power Model</i>	67
<i>Experimental Results and Conclusion</i>	69
Appendix A – MATLAB Model Code for Tm:Germanate	72
Appendix B – ZEMAX Pump Design Procedure	75
Appendix C - Pump Chamber Alignment Procedure	79
Appendix D – Mechanical Drawings	84
Parabolic Mirror.....	84
Parabolic Mirror Mounting Bracket	85
Thin Disk Heatsink	86
Thin Disk Water Adapter.....	87
References	88

List of Figures

1.1	Rectangular thin slab concept [5].....	2
1.2	Zig-Zag thin slab laser concept [5].....	3
1.3	Schematic view of the thin disk laser design [15].....	4
1.4	Power output from a single disk Trumpf Yb:YAG thin disk laser [15].....	5
1.5	Schematic view of the thin disk laser pumping scheme [8].....	6
1.6	Thin Disk Module TDM 1.0 SMA courtesy of Dausinger+Guisen GMBH.	6
1.7	Absorption of water [17].....	7
1.8	Thulium energy level scheme.....	10
1.9	Thulium Germanate cross-section absorption and emission curves [12]....	10
2.1	Essential laser components.....	13
2.2	Elements of a Thin Disk Laser.....	14
2.3	Doping atoms in a host material.....	15
2.4	Wavelength emissions for various gain materials [5].....	16
2.5	Thin disk laser various cavity configurations.....	18
2.6	Example of thin disk module stacking for high output power.....	19
2.7	Common stable resonator configurations [5].....	20
2.8	Thin disk pump scheme using Non-Sequential Zemax.....	21
2.9	Two-dimensional thin disk pump concept.....	22
2.10	Thin disk's four fold mirrors beam directions.....	23
2.11	Source optics into pump chamber.....	24
3.1	Absorption and emission interactions.....	26
3.2	Three level diagram of Thulium.....	29
3.3	Simplified energy level diagram of Thulium.....	32
3.4	Gain and absorption of the gain material.....	34
3.5	Linear cavity signal ray propagation for gain threshold.....	35
3.6	Pump light losses as beam folds around pump chamber.....	37
3.7	Aperture effect of pump focus in thin disk laser.....	40
3.8	Power Output vs Power Input for theoretical and measured data of the Yb:YAG laser.....	43
4.1	Pump source in designed system.....	47
4.2	Collimation optics in designed system.....	47
4.3	Parabolic mirror.....	48
4.4	Fold mirrors in designed system.....	48
4.5	Interferometer measurements using a WYKO 6000.....	49
4.6	Tm:Germanate thin disk in designed system.....	49
4.7	Thin disk heatsink copper piece.....	50
4.8	Thin disk heatsink water cooling process.....	50

4.9	Thin disk heatsink and cooling apparatus.....	50
4.10	Tm:Germanate resonator configuration.....	51
4.11	Solidworks model of pump module.....	52
4.12	Solidworks model of pump optics.....	52
4.13	Non-Sequential Zemax Layout (view 1 and 2).....	53
4.14	Non-Sequential Zemax Layout of 20 beams.....	53
4.15	Real System layout.....	54
4.16	Pump optics layout (zoomed in).....	54
4.17	Pump chamber alignment using an interferometer as a large diameter collimator.....	55
4.18	Parabolic mirror and thin disk alignment concept.....	56
4.19	Pinhole misalignment characteristics for parabola to thin disk alignment...	57
4.20	Thin disks four fold mirrors alignment concept.....	58
4.21	Angle adjustment of four fold mirrors.....	59
4.22	Source optics alignment concept.....	60
4.23	Prototype of source optics and pump chamber.....	61
4.24	Source optics beam alignment characteristics.....	61
4.25	Resonator alignment concept.....	62
5.1	Zemax modelled data from a DILAS 793nm fiber diode.....	64
5.2	Pump spot's cross section at the thin disk focus.....	65
5.3	Pump spot on thin disk HR side (zoomed in).....	66
5.4	Comparison of pump spot on thin disk HR side.....	66
5.5	Tm:Germanate power output vs power input for various s-p coupling values.....	68
5.6	Pump spot temperature experience in thin disk.....	69
5.7	Tm:Germanate thin disk temperature vs power input for various interface materials.....	70
5.8	Pump spot temperature in Yb:YAG thin disk laser.....	71

List of Tables

2.1	Effects of different host materials using Thulium [2].....	17
3.1	Dausinger-Guisen Yb:YAG system parameters for modelling.....	42
3.2	Comparison of the slope efficiency and signal pump coupling values.....	44
3.3	Model Verification using Threshold Difference.....	44
4.1	Summary of first order Tm:Germanate design.....	46
5.1	Tm:Germanate Model Parameters.....	67
5.2	Threshold and slope efficiency values for various s-p coupling values.....	68

Abstract

A Thulium Germanate thin disk laser prototype is developed and its potential applications are discussed. Unfortunately, the thin disk gain material for the CW prototype was unable to lase due to thermal limitations within the glass. However, a CW output power model and a physical pump chamber module have been developed, along with the supporting Zemax models and alignment procedures so other gain materials and future improvements can be tested.

Chapter 1

Introduction

For several decades, laser designs have greatly evolved to accommodate the demand for higher power, smaller size, better efficiency, and lower input power requirements. In the past 17 years, thin disk lasers have been of particular interest due to its ability to meet these increasing demands while allowing moderate costs for manufacture, power scalability, and good output beam quality [1].

Furthermore, thin disk lasers have the ability be scaled to large powers and to use a wide range of gain materials for various wavelength output emissions. In particular, the 2 μ m region is of interest due to laser sensing/spectroscopy, medical applications, material processing, free space optical communications, and military applications [2].

This thesis presents the design and manufacture of a prototype CW thin disk laser using Thulium-Germanate as a prototype for further research and development. Future experiments using different active gain media and enhanced laser techniques such as Q-switching and Mode-Locking can be used with the manufactured design.

1.1 History

The LASER, which is an acronym for Light Amplification by Stimulated Emission of Radiation, was first demonstrated by Theodore Maiman in 1960 using Ruby. Since then, lasers have gone through revolutionary changes and have developed into countless design configurations using different kinds of atoms, molecules, and ions, in the form of gasses, liquids, crystals, glasses, plastics, and semiconductors [4]. Of the various designs invented, each has suffered its own set of limitations such as inadequate power, damage in the gain medium, poor beam quality, and erratic mode behavior. To combat such issues and improve solid-state laser capabilities, initial designs went through multiple iterations using unique configurations. Nevertheless, all designs encompass the same basic physics of stimulated and spontaneous emission first theorized by Einstein in 1917.

Rectangular Thin Slab Laser

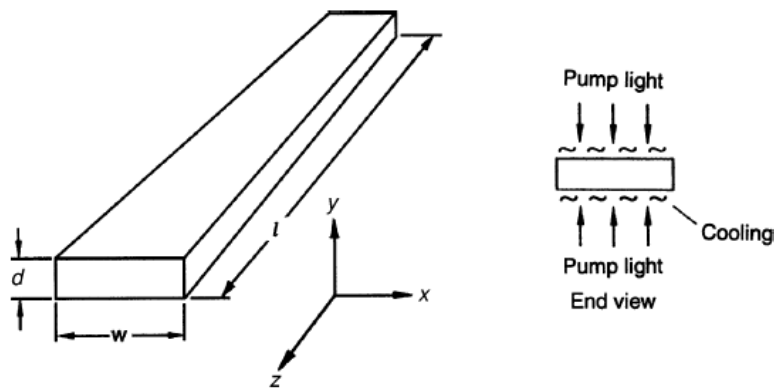


Figure 1.1 Rectangular thin slab concept [5].

Before the thin disk laser, one of the first improvements started as a thin slab laser utilizing both sides of the gain medium pumped with light. This design improved on existing bulk rod designs by giving a larger cooling surface and twice the pump power. In return, this gave the system more laser power and a one-dimensional temperature gradient across the thickness of the slab [5]. Unfortunately, this design had low performance once pump powers were increased since the slab would experience large thermal lensing and eventually fracture. This led to catastrophic failure and limited the scalability of the design.

Zig-Zag Thin Slab Laser

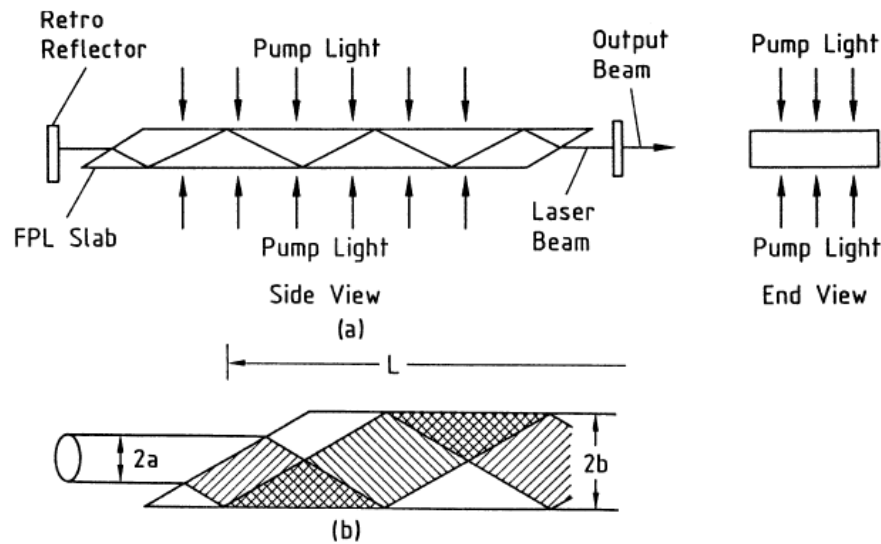


Figure 1.2 Zig-Zag thin slab laser concept [5].

The next improvement of the thin slab design was by Martin and Chernoch using heatsinks on the sides of the gain medium, as well as a zig-zag active lasing beam pattern instead of a linear beam path. The zig-zag pattern reduced thermal lensing due to the optical path being averaged across the thermal gradient, and

also minimized stress induced birefringence due to the rectilinear cross section [9]. However, the design was limited by residual distortions at the slab ends and pump faces, as well as mechanical mounting complications, low efficiency, and high fabrication costs [5]. Also, the thickness and cooling efficiency was greatly decoupled causing large variations in one parameter when the other was slightly modified.

Thin Disk Laser

To further improve thin slab lasers, researchers at the University of Stuttgart in 1994 published a new way to mount a round thin slab (thin disk) to a heatsink and pump the disk axially.

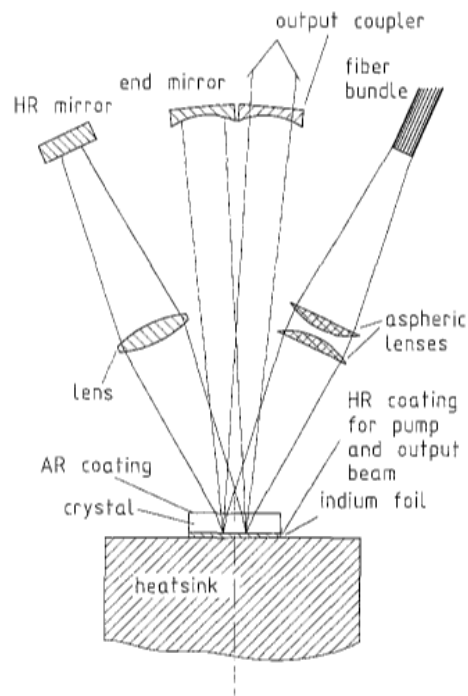


Figure 1.3 Schematic view of the thin disk laser design [15].

In this design configuration, the active gain medium has a thickness ranging from 100 μm to 500 μm with a disk diameter ranging from 5mm to 10mm [23]. The surface mounted to the thin disk is coated with a highly reflective coating and serves as one of the resonator mirrors. Heat in the thin disk is extracted one-dimensionally along the optical axis directly to the heatsink, which efficiently removes the heat generated from the pump source and active lasing region. This ultimately minimizes stresses, radial thermal gradients, and refraction index variations, especially when the thickness is relatively small compare to the thin disk's diameter [5]. This novel concept allows the laser to obtain kilowatts of average power at room temperature while maintaining good beam quality, ideal pulse characteristics, and high efficiency [15].

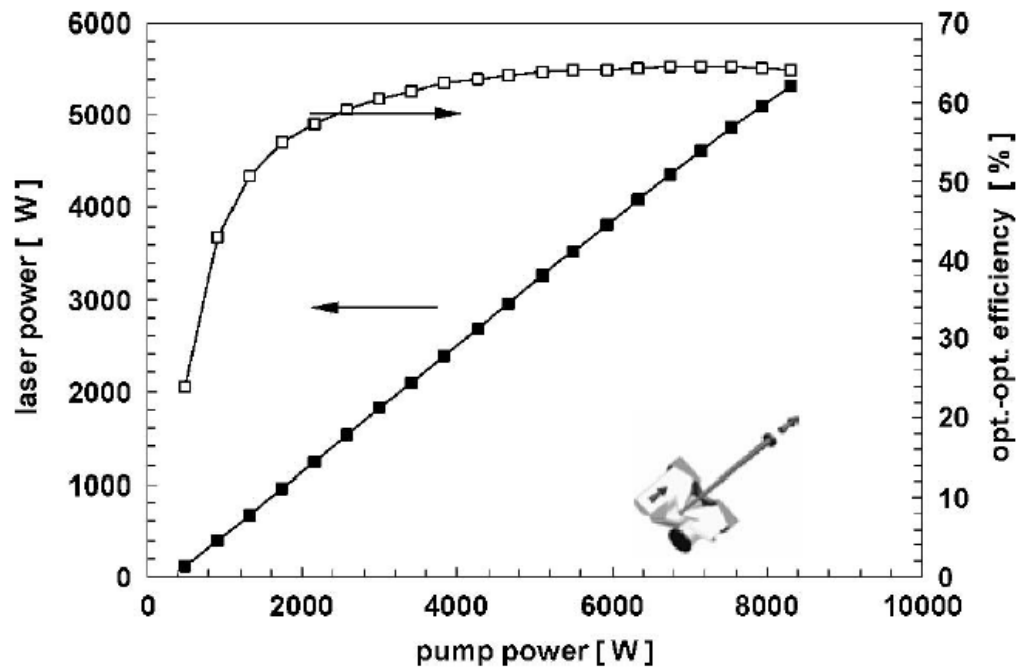


Figure 1.4 Power output from a single disk Trupf Yb:YAG thin disk laser [15].

To achieve such high output powers, multiple passes through the thin disk are required. This is done by using a single source laser and creatively coupling it with several optical elements to fold the beam multiple times over the same spot. This allows the gain medium to experience high source powers typically ranging from 6 to 20 times the initial source power.

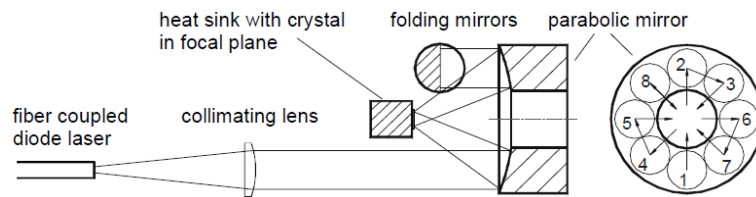


Figure 1.5 Schematic view of the thin disk laser pumping scheme [8].

The thin disk laser module can also be a very compact system for the power output. As can be seen below in figure 1.6, the Dausinger-Guisen module has dimensions of 311mm x 122mm and uses the supporting housing to efficiently cool the system. Using the same pump power density, the system can host a wide range pump powers up to 250W by simply scaling up the spot size.

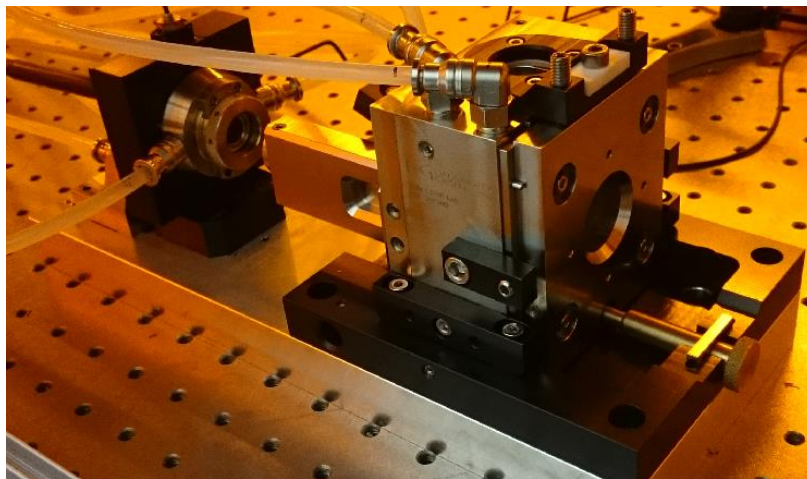


Figure 1.6. Thin Disk Module TDM 1.0 SMA courtesy of Dausinger+Guisen GMBH.

1.2 Areas of Interest

The regions of 450nm to 550nm and 1860nm to 1945nm are of interest due to its low and high absorption peaks in water. Other materials are also of interest due to their high absorption peaks near 2 μ m. This provides the ability to advance new technologies not available in the past from lack of power and capability.

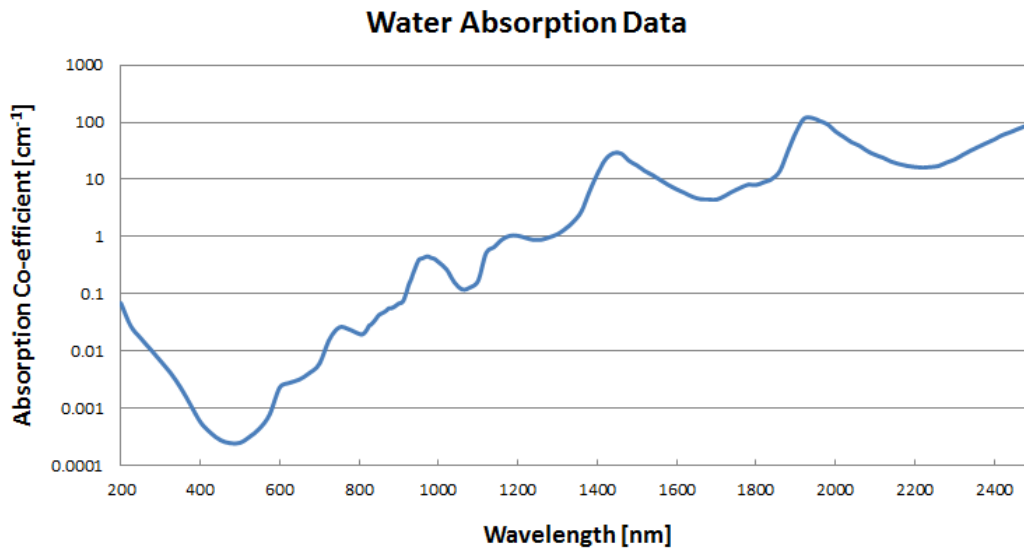


Figure 1.7 Absorption of water [17].

Military Applications

- Eye Safe Targeting Devices - Many incidents have been reported from battlefield conditions and unsafe use where users are blinded by a friendly laser sweeping across a combat zone [16]. Water in the vitreous portion of the eye heavily absorbs the 2 μ m wavelength region and prevents damaging radiation from injuring the retina. This is particularly ideal for

small unit laser systems such as designators and IR targeting systems, where the lasers can be pointed at other friendly soldier's faces.

- LIDAR and Scanning Systems - Multilevel harmonic generation can be used to obtain a wavelength near 475nm. In this wavelength region, light is least absorbed by water. This creates the potential for mapping underwater regions for detection of submarines, mines, combatants, and other debris [2].

Medical Applications

- High Absorption and Low Penetration Depth – Once again, as an application due to high absorption in water, the 2 μ m laser provides the ability for high precision surgical processes for both soft and hard tissues [2]. Compared to other laser wavelengths, 2 μ m laser radiation helps to suppress bleeding during surgical operations and limits heat induced damage in the surrounding tissue.

Material Processing

- Plastic Cutting, Welding, and Marking – Since existing weldable plastics are highly transparent near the 1 μ m region, they need very high CW powers and must be mixed with additional compounds to make the plastic weldable [2]. Wavelengths around 2 μ m are highly absorbed in many plastics. This provides the ability to weld existing plastics with high quality joints and limit the amount of toxic substances released during the welding process.

Laser Sensing and Spectroscopy

- Element and Atmospheric Detection – A number of atmospheric gases such as water, carbon dioxide, and nitrogen oxide all have absorption lines near the 2 μ m region. Using CW and pulsed systems, these gases can be used to detect and analyze atmospheric conditions [2].

1.3 Thulium Germanate Thin Disk as Potential

Since the thin disk architecture has only been discovered in the past 17 years, new materials have not been extensively investigated yet. Other host materials such as Tm:YAG, Tm:YLF, and Tm:YAP have been used, but they have shown limitations such as birefringence, low damage threshold, or high manufacturing costs.

One such material to meet increasing requirements is Thulium Germanate; unfortunately it is a fairly new material and there is no information about its use as a thin disk laser. Comparatively, Tm³⁺ doped crystals in fiber platforms have shown great benefits such as its high efficiency and long radiative lifetimes [2]. Germanate glass has also shown great benefits as a host matrix due to its combination of good thermal stability, high solubility, low phonon energy, lack of birefringent dependence, and high transparency in a wide wavelength range [10].

Thulium Germanate as Gain Medium

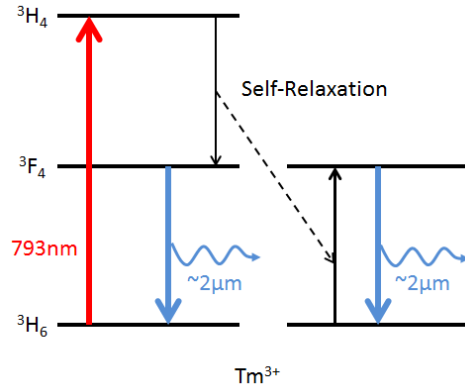


Figure 1.8 Thulium energy level scheme.

Pump radiation at 793nm transfers Tm^{3+} ions from the 3H_6 ground state into the 3H_4 pump state. At this point, the excitation undergoes a transition from 3H_4 to 3F_4 , while an unexcited ion undergoes a transition from 3H_6 to 3F_4 due to a self-relaxation process. Ultimately, this process creates two ions in the upper state for every one photon absorbed, giving a quantum efficiency of 2.

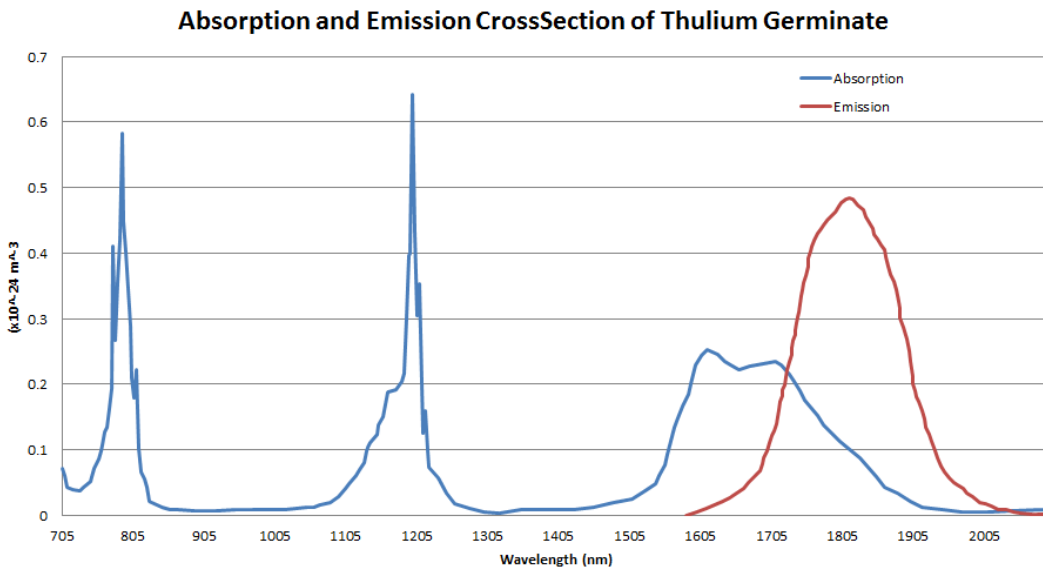


Figure 1.9 Thulium Germanate cross-section absorption and emission curves [12].

According to measured data from NP Photonics, Thulium Germanate has an ideal emission wavelength region of 1600 to 2000nm, and also has a high absorption peak wavelength of 793nm. The emission spectrum meets the requirements for many applications, and the absorption wavelength is ideal since Thulium Germanate can be pumped by an easily obtainable commercial fiber laser module at 793nm. Also, germanate glass as a host has shown lower phonon energy (900 cm^{-1}) compared to silica glass (1100 cm^{-1}) which helps to increase the quantum efficiency and reduce the non-radiative decay rate of the upper lasing level of 3F_4 [24]. Germanate can also be doped much higher due to its higher solubility of Thulium from a lower quenching effect [25].

Thulium Germanate as a Thin Disk Laser

Quasi-three-level materials have shown the highest efficiency in thin disk lasers, but can be difficult to operate because the laser wavelength experiences high absorption from the ground state being so close to the lower laser level [7]. This requires high pump intensities and low temperatures in the crystal to achieve laser threshold. Thulium Germanate, a quasi-three-level material, gives the opportunity to achieve such high efficiencies, but risks experiencing high temperatures inside the material. Using Thulium Germanate in a thin disc system can obtain very high powers by utilizing the heat sink and by scaling the pump diameter similar to other Yb:YAG thin disk lasers. It can also be used as a high energy system due to the short gain medium making it ideal for Q-switching and mode-locking. This is of high interest and would provide a great improvement over currently limited fiber systems.

1.4 Motivation and Intent

The desire to design and manufacture a working prototype of a Thulium Germanate thin disk laser is of high importance. Such a device can open up new research opportunities and create the ability to enhance areas in laser sensing and spectroscopy, medical applications, material processing, and military applications.

The prototype system will have a broadband high reflection coating centered around 795nm on the pump chamber optics. This coating region allows for investigations into other host materials whose absorption wavelength falls around this value. Having the capability to investigate different host materials gives the option to develop new technologies and expand further research.

Also, the prototype was designed to be a cheap experimentation version to study of the characteristics within the thin disk architecture. The prototype is not meant as a final product and is intended to learn many aspects of the design. Having a starting prototype allows for cost efficient investigations into heating effects, pumping characteristics, lasing parameters, and issues not yet encountered. Learning these parameters enhances future iterations so a newer system can be more robust, obtain higher powers, have better efficiency, as well as provide the opportunity to experiment with Q-switching and mode-locking techniques. Without a CW prototype to investigate, none of this is possible.

Chapter 2

Thin Disk Laser Basics

Simply put, lasers are basically a light amplifier utilizing its own light as feedback. Many designs utilize different configurations, but all utilize the same basic physics and have 3 essential components; the laser gain medium to amplify light, an oscillator configuration for optical feedback, and pump light to induce population inversion in the gain medium.

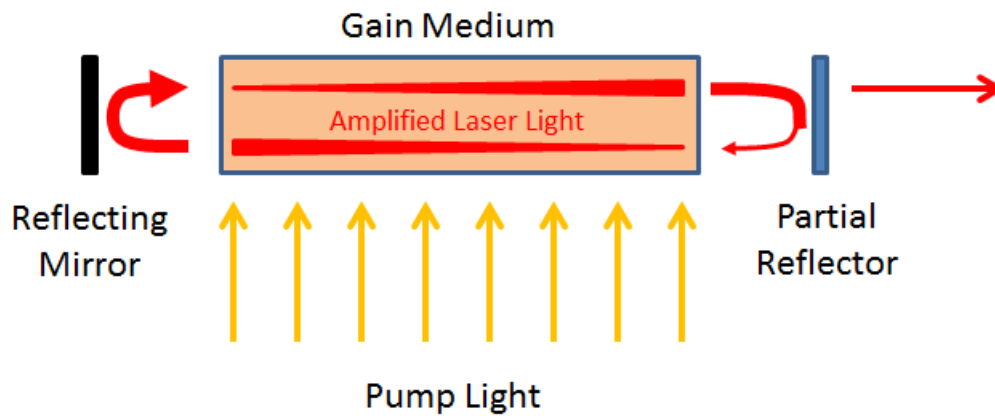


Figure 2.1 Essential laser components.

As can be seen in figure 2.2 below, the thin disk laser incorporates multiple components; however, the laser system only differs by physical dimensions and pumping scheme. Nothing is different from the core principles of a laser.

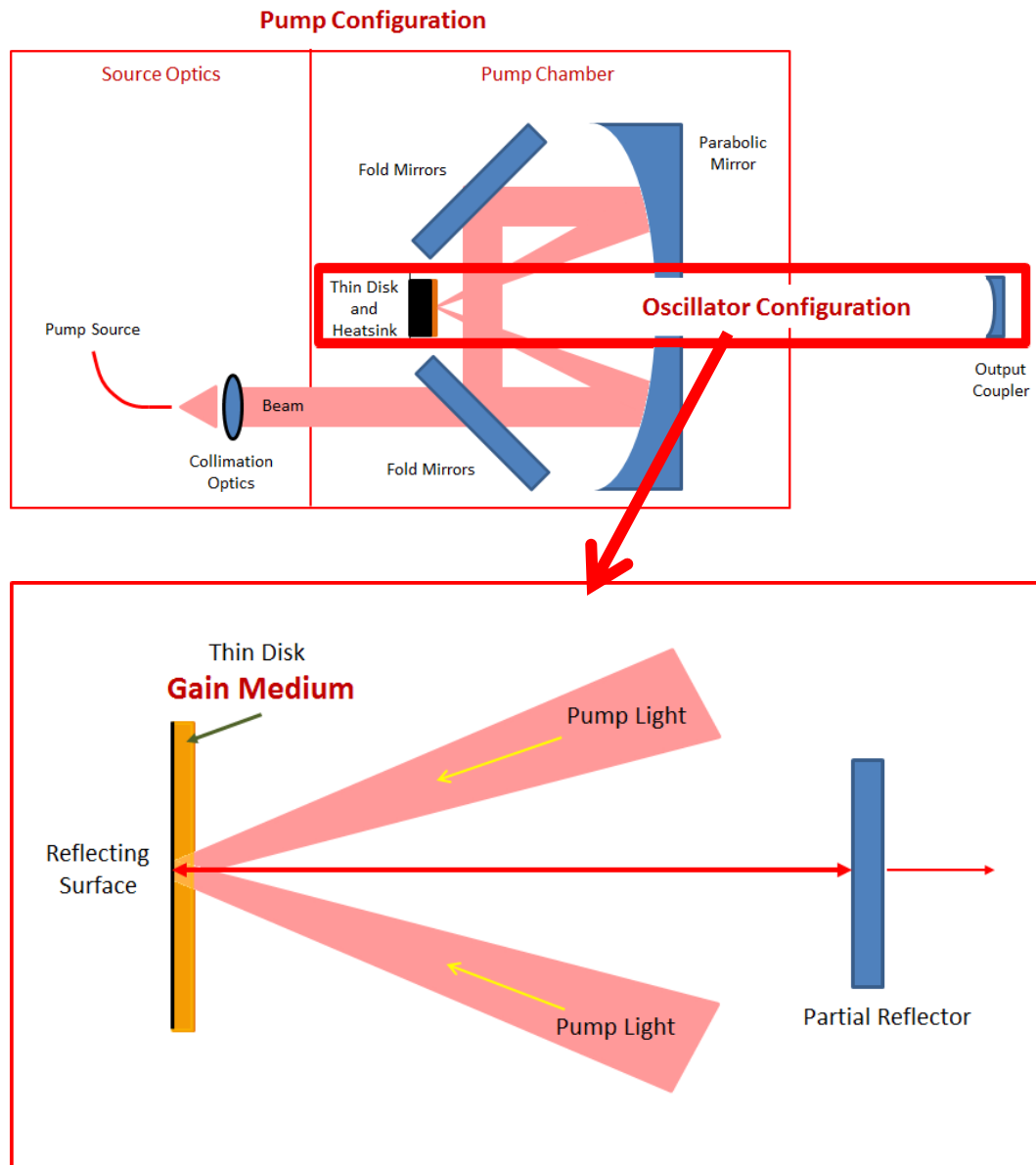


Figure 2.2 Elements of a Thin Disk Laser.

2.1 Laser Gain Medium

The laser gain medium is a collection of atoms, molecules, ions, or semiconductor electrons. These can take the form of liquids such as organic dye rhodamine 6G, gasses such as the Helium Neon, atoms doped in a host crystal such as Nd:YAG, or semiconductor form such as Gallium Arsenide. For the thin disk laser design, the amplifying gain medium is atoms doped in a glass/crystal matrix. This is considered a solid-state system in this configuration.

Amplifying Atoms

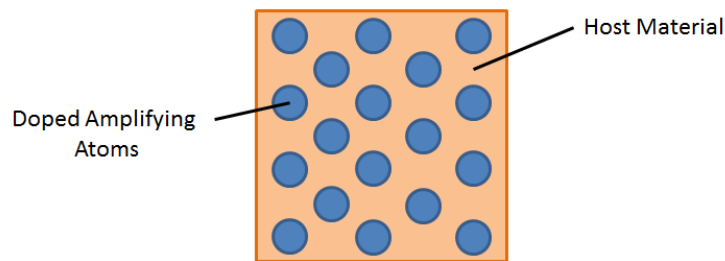


Figure 2.3 Doping atoms in a host material.

Generally, in a solid-state laser's gain medium, trivalent rare earth atoms such as Ytterbium³⁺, Erbium³⁺, or Neodymium³⁺ (in this thesis, Thulium³⁺) are doped inside a host material such as such as Sapphire, Silica or YAG (in this thesis, Germanate). The doped atoms enable the crystal to amplify light through the process of stimulated absorption and emission, with each type of atom having excited state transitions determined by the quantum nature of the doped atom. Rare earth atoms are generally used because the electrons in the partially filled 4F shell can be raised to unoccupied 4F levels by absorption of light.

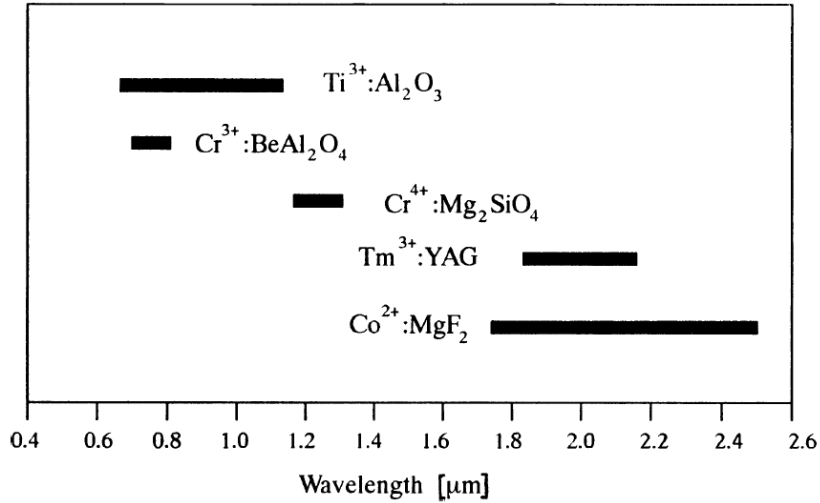


Figure 2.4 Wavelength emissions for various gain materials [5].

Thin disk lasers preferably use quasi-three level atoms such as Ytterbium, because the pump power necessary for maintaining inversion is small and they have shown the highest optical efficiency, good beam quality, highest output power characteristics, and best thermal management from lower thermal loading factors [26]. However, because of the ground state being so close to the transitioning state, it has required large pumping powers to reach threshold.

Typically, the doped atoms are reported as a percentage paired with the number density, N , of laser active ions per unit volume. This is the most convenient notation for calculating various laser parameters since many other calculations use the number of atoms per unit volume such as rate equations and cross section values. Typically, doping ranges for solid state systems are on the order of 1% to 3% [5]. In thin disk systems however, doping concentrations are generally higher around 5% up to 30% for some Yb:YAG systems [18].

Host Material

The host material, in which the amplifying atoms are doped in, is used as a means to fix the doping atoms in various configurations and densities in space. The host crystal usually consists of a highly transparent material associated with the absorption and emission wavelength of the doped atoms. Typically, it's uniformly homogenous and depending on the application, the doped atoms can be doped with various percentage levels to influence laser beam output characteristics.

As mentioned earlier, doping levels are usually higher in thin disk systems and the host needs to be able to support the higher doped levels. Properties of the host crystal need to encompass multiple characteristics such as hardness, damage threshold, polarization, and solubility. As seen in the chart below, the host material has an effect on the doping atoms by influencing the wavelength, bandwidth, absorption and emission cross sections, radiative lifetimes, and non-radiative transitions.

laser host material	σ_{abs} (10^{-21} cm^2)	λ_{em} (nm)	σ_{em} (10^{-21} cm^2)	λ_{th} ($\text{W m}^{-1} \text{ K}^{-1}$)	τ (ms)	reference
YAG	7.5	2013	1.8	13	10	Heine, 1995
YLF	σ pol 3.6 π pol 8.0	1910 1880	2.35 3.7	6	15.6	Payne et al., 1992 Walsh et al., 1998
Lu ₂ O ₃	3.8	2070 1945	2.3 8.5	13	3.8	Koopmann et al., 2009a
Sc ₂ O ₃	5.0	1994	8.4	17	4.0	Fornasiero et al., 1999
Y ₂ O ₃	5.0	2050 1932	2.1 8.1	14		Ermeneux et al., 1999
LuAG	5.7	2023	1.66	13	10.9	Scholle et al., 2004
YAlO ₃		1936	5.0	11	4.8	Payne et al., 1992
silica fibre	4.5	1860	3.9		6.6	Agger & Povlsen, 2006
germanate f.	6	1840	4.1		5.3	Turri et al., 2008

Table 2.1 Effects of different host materials using Thulium³⁺ [2].

2.2 Laser Oscillator

The laser oscillator is the configuration in which mirrors return light to enable amplification of the laser signal and also determine resonator modes. As a bare minimum, two mirror surfaces are needed; a highly reflective surface and a partially reflective surface. The high reflection's purpose is to reflect internal resonating light back for amplification at minimal losses so higher laser output is achieved. The partially reflecting mirror, commonly referred to as an output coupler, is used to allow some of the laser light to escape the system while the reflected light is sent back into the resonator to be amplified again. Eventually, the laser's amplification and internal losses from the mirrors reach an equilibrium point and the escaped laser light becomes a steady beam output.

Cavity Configurations

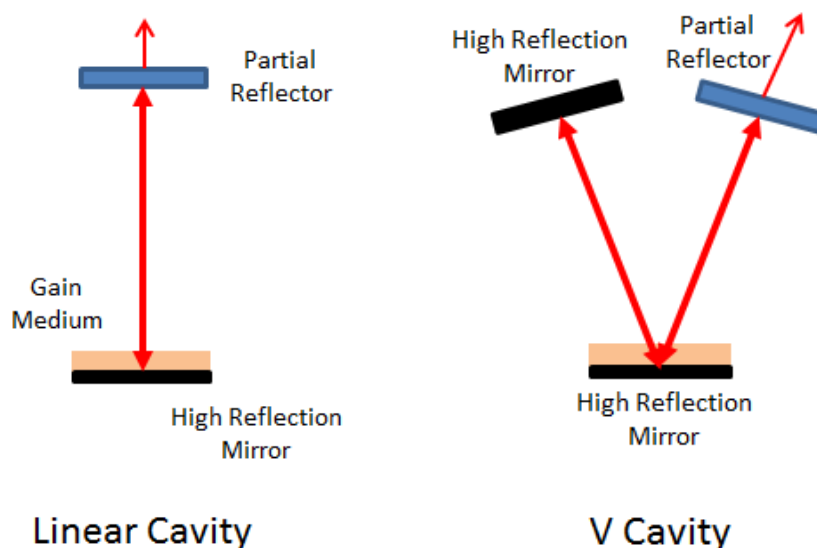


Figure 2.5 Thin disk laser various cavity configurations.

In a thin disk laser, two cavity configurations are used; the linear cavity configuration and the V-cavity configuration. In a linear cavity, the laser signal resonates back and forth along the axis of the laser system and has a double pass through the gain medium for each round trip. In a V-cavity configuration, a separate end reflector is used causing the beam to be decoupled from the high reflection side of the thin disk. In this configuration, the beam passes four times through the gain medium per round trip, which gives the most amplification per resonating loop. Both configurations can be used to stack several thin disk modules to achieve high amplification and output powers.

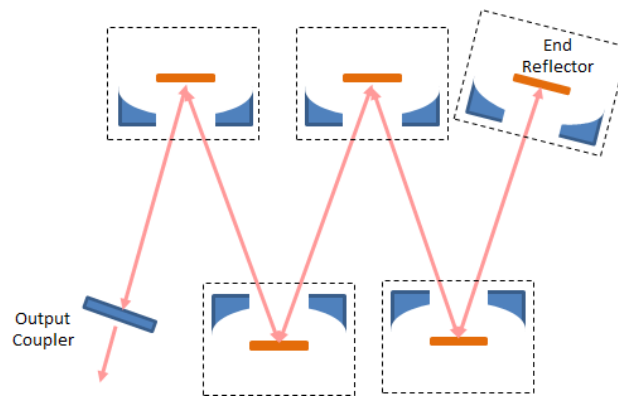


Figure 2.6 Example of thin disk module stacking for high output power.

Resonator Types

There are two types of laser resonators; a stable resonator and an unstable resonator. Stable resonators are described as the resonator mirror configuration that allows the resonating ray to continuously stay in the cavity. These two mirrors essentially couple the oscillating Gaussian wave so the signal light is continuously amplified. If a small portion of the photons are lost out of the

resonator from misalignment, diffraction, or other scattering effects; the output power decreases since the photons are no longer able to be amplified. We can consider the loss as a loss factor for coupling of the signal light to amplified medium.

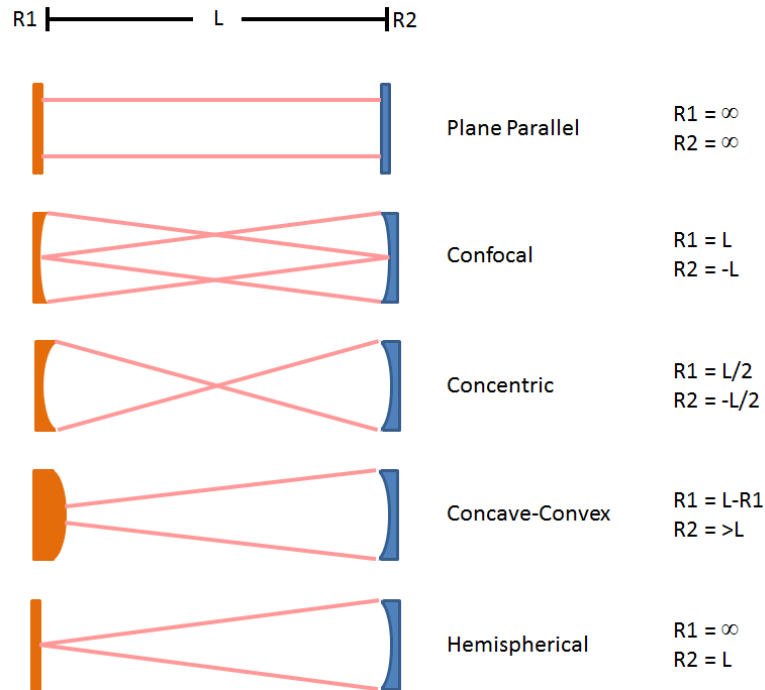


Figure 2.7 Common stable resonator configurations [5].

Unstable resonators are oriented such that the resonating ray eventually leaves the resonating path (diverges) and is no longer part of the amplifying path. While there are benefits to such a configuration such as lower divergence, they are not of interest in this thesis since the misalignment tolerance of an unstable resonator is smaller compared to its stable counterpart [5].

2.3 Pumping Configuration

The pumping configuration is used as a means to send pump light into the gain medium. Sources can take the form of flash lamps, seed laser systems, or diode emitted lasers. In the case of the thin disk laser, one laser source is used in combination with other optics to focus one beam into multiple overlapped beams to increase power on the thin disk.

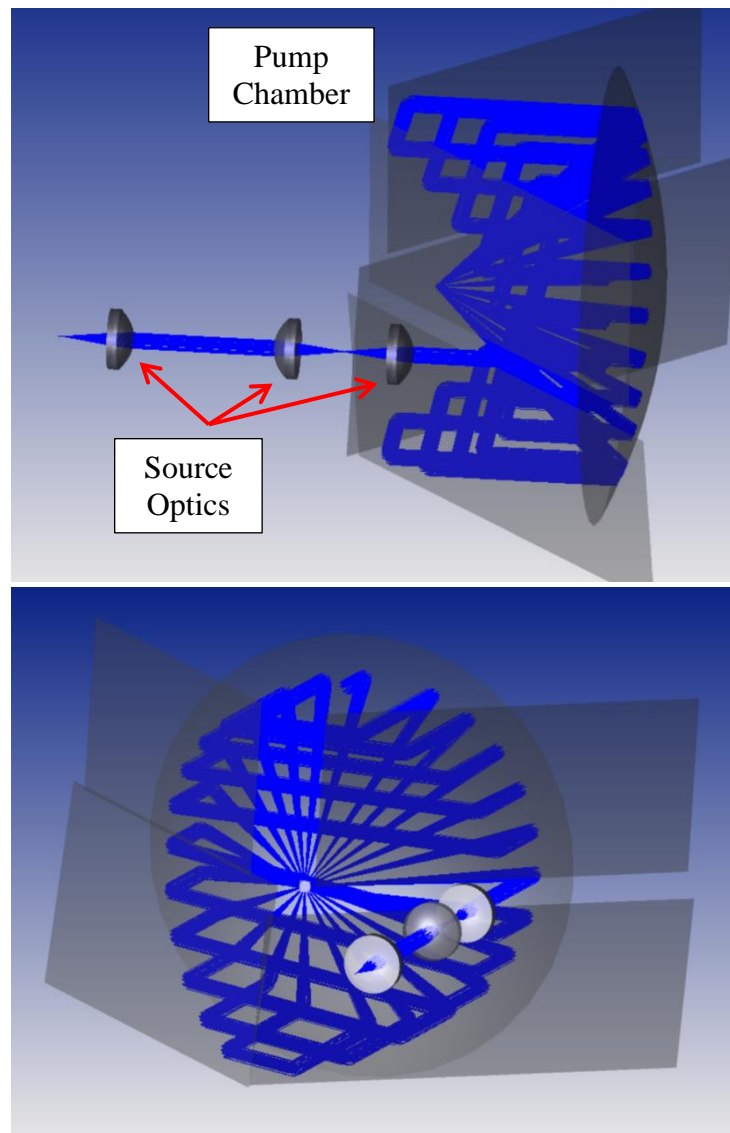


Figure 2.8 Thin disk pump scheme using Non-Sequential Zemax.

Pump Chamber

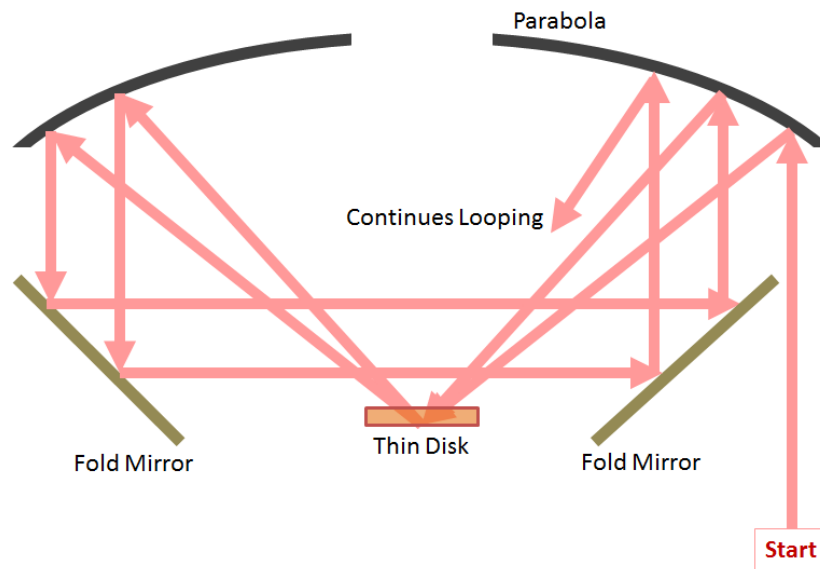


Figure 2.9 Two-dimensional thin disk pump concept.

In the thin disk configuration, a parabola and four fold mirrors are used to focus a collimated fiber laser beam onto the thin disk for maximum use of a source laser. As can be seen in figure 2.8, a source, generally a fiber laser, emits a narrow band light and is collimated by a set of lenses. The collimated beam then travels to the parabola where it is focused down to the thin disk. At this point, the thin disk absorbs and reflects the pump light back to the parabola. The parabola reflects and collimates the beam to the fold mirrors. The fold mirrors change the beam's location so it comes in collimated to the parabola again, only at different locations on the parabola. This propagation continues for a designed number of times or until the pump light has diminished due to absorption from the thin disk and reflection losses.

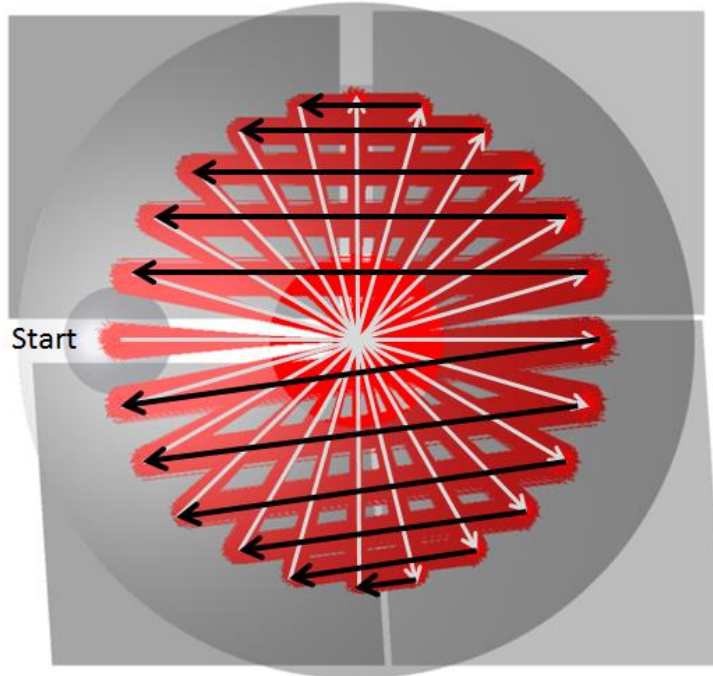


Figure 2.10 Thin disk's four fold mirrors beam directions.

The four fold mirrors control how the beam is folded to be on-axis to the parabolic mirror. More specifically, the two bottom mirrors are tilted and translated so the beam's on-axis locations are changed on the parabolic mirror. This determines the number of passes that go through the thin disk and the number of spots located on the parabola. As seen above in figure 2.10, the black lines show the beam path caused by the fold mirrors, while the gray lines show the beam path caused by the parabola and thin disk. The two top mirrors are simply oriented at 45 degrees to fold the beam horizontally, and the translation position determines the spot location on the parabola. Same goes for the two bottom mirrors except that the angle is also directed in both the X and Y directions to set the number of spots on the parabola.

Source Optics

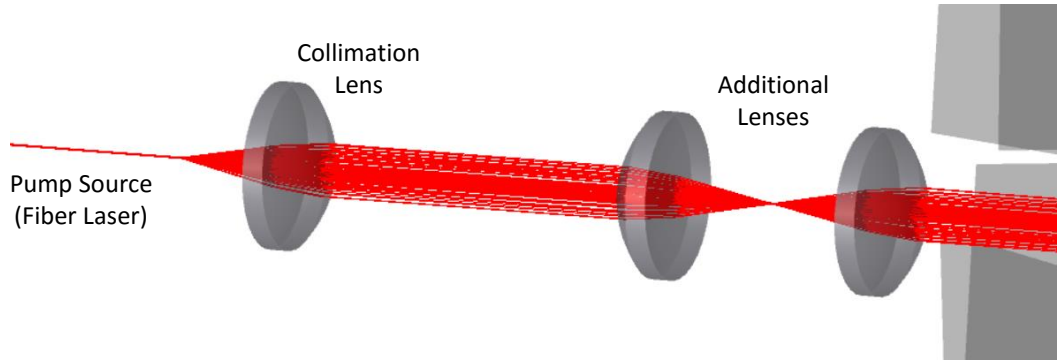


Figure 2.11 Source optics into pump chamber.

An initial pump source is used in combination with collimating optics before projecting into the pump chamber. For the thin disk laser, compact systems use fiber diode lasers; however other ‘seed’ lasers can be used to send a specific laser into the gain medium. The collimation optics can be as simple as a single lens, or can be a combination of lenses for alignment purposes or to minimize aberrations.

In compact thin disk systems (shown in figure 1.6), a fiber laser emits light to a lens where the light is then collimated to two additional lenses. The additional lenses are typically used for alignment purposes such as accurate translation of the incoming beam and to possibly change magnification before entering the pump chamber.

Chapter 3

Laser Fundamentals and Modelling

Fundamentally, operation of a laser can be described and modeled from absorption and emission processes. Detailed quantum models and specific interaction effects of atoms are not required. As a basis, the only required knowledge is that there are discrete energy levels between states of electrons in an atom; and that each atom has its own allowed electron transition states defined by the quantum numbers associated with the atom. These electrons can be excited to higher energy levels by absorption through various excitation processes, and then transition back down to lower energy levels by the emission of photons through spontaneous emission, stimulated emission or other quantum mechanical phenomenon.

3.1 Light Interactions

Simply, a two level energy diagram can be used to describe the multi-level states in an atom; a ground state $|1\rangle$ with energy E_1 , and an excited state $|2\rangle$ with

energy E_2 . Using Plank's Law, the energy difference between the two states is given by the relation,

$$\Delta E_{\text{photon}} = h\nu = E_2 - E_1 \quad (3.1)$$

where h is planks constant ($6.626 \times 10^{-34} \text{ m}^2 \cdot \text{kg} \cdot \text{s}^{-1}$), c is the speed of light ($3 \times 10^8 \text{ ms}^{-1}$), and ν is the frequency of the light. To give a statistical indication of the population of atoms either in the excited state or ground state at thermal equilibrium, the Boltzmann ratio is used and is related by,

$$\frac{N_2}{N_1} = e^{\frac{-(E_2 - E_1)}{kT}} \quad (3.2)$$

where N_1 and N_2 describe the population density in each state, k is the Boltzmann constant ($1.38 \times 10^{-23} \text{ m}^2 \cdot \text{kg} \cdot \text{s}^{-2} \cdot \text{K}^{-1}$), and T is the temperature in Kelvins. If light is coupled to an atom, three different types of interactions can take place; spontaneous emission of light, absorption of the light, or stimulated emission from light.

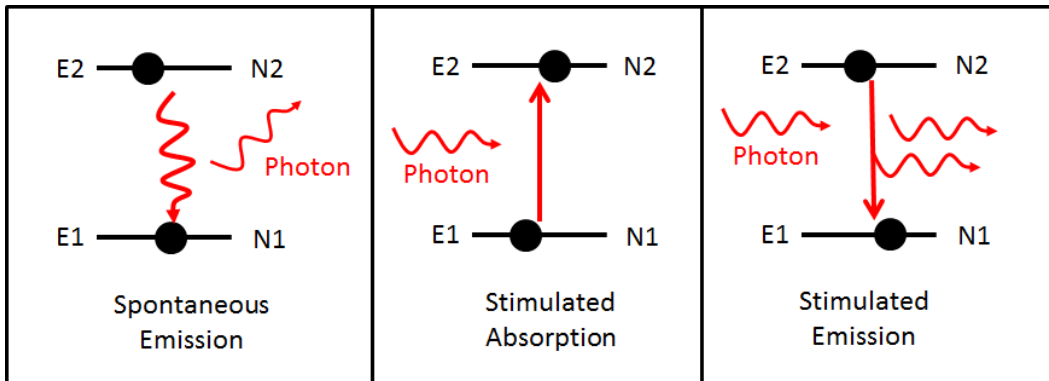


Figure 3.1 Absorption and emission interactions.

Spontaneous Emission

Atoms in the upper state $|2\rangle$ will spontaneously emit radiation back to the ground state $|1\rangle$ at a rate described by Einstein's relation,

$$\frac{\partial N_2}{\partial t} = -A_{21}N_2 = -\frac{N_2}{\tau_{21}} \quad (3.3)$$

where A_{21} is the constant of proportionality, and τ_{21} is the radiative lifetime. This gives the transition probability that an atom in the excited state will spontaneously emit a photon and transition to the ground state within a unit of time. Light that is emitted in this fashion is incoherent with no phase relationship and can generally be described as the fluorescence of a material.

Absorption

Photons with energy E that pass through ground state atoms with similar energy to the ΔE between the ground state and excited state, will be absorbed and induce an upward electron transition at a rate defined by,

$$\frac{\partial N_1}{\partial t} = -B_{12}\rho(\lambda_{12})N_1 = -\sigma_\lambda^a \frac{I_\lambda}{(h\nu)} N_1 \quad (3.4)$$

where $-B_{12}$ is the constant of proportionality and $\rho(\lambda_{12})$ is the radiation energy density. These two variables provide the probability of transitioning the population density N_1 . This can also be related by the photon density $(\frac{I_\lambda}{h\nu})$ times the cross-section absorption value (σ_λ^a) for that specific wavelength of light.

Stimulated Emission

Photons with energy E that pass through excited state atoms with energy similar to ΔE between the excited state and ground state, will cause the atoms to release their energy as a photon similar to the passing photon. Light that is emitted in this fashion is coherent and has the same phase/polarization as the incident photon. This rate of stimulated emission is determined by the relation,

$$\frac{\partial N_2}{\partial t} = -B_{21}\rho(\lambda_{21})N_2 = -\sigma_\lambda^e \frac{I_\lambda}{(h\nu)} N_2 \quad (3.5)$$

where $-B_{21}$ is constant of proportionality and $\rho(\lambda_{21})$ is the radiation energy density. Once again, these two variables provide the probability of transitioning the population density N_2 . This can also be related by the photon density $(\frac{I_\lambda}{(h\nu)})$ times the cross-section emission value (σ_λ^e) for that specific wavelength of light.

3.2 Laser Operation

Lasers use the three processes described above, but purely as a two-state system, lasing cannot occur due to absorption and spontaneous emission always exceeding stimulated emission. Therefore, pumping to a higher energy level with a more energetic wavelength is required so the process can fill a metastable state, in which the system can obtain 'population inversion'. This is when stimulated emission exceeds absorption and spontaneous emission processes.

Three Level System

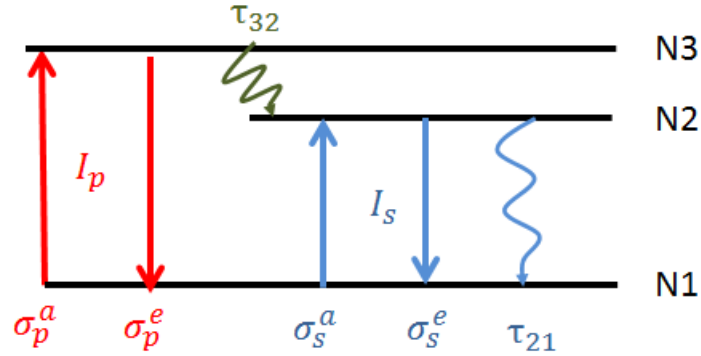


Figure 3.2 Three level diagram of Thulium.

For Thulium, the energy level diagram is considered a three-level system, which is simplified to a ground state $|1\rangle$, a metastable state $|2\rangle$, and a pumping state $|3\rangle$. In this scheme, pump light I_p incident on the gain medium is absorbed a and emitted e at a value determined by the cross-section σ of the gain material. The absorbed power transitions atoms to state $|3\rangle$, where it then transitions very fast into state $|2\rangle$ at a rate defined by τ_{32} . At this point, atoms in state $|2\rangle$ transition to state $|1\rangle$ by emitting photons as stimulated emission of the signal light I_s or as spontaneous emission at a rate defined by τ_{21} . Also, a portion of the signal light is re-absorbed. Lasing begins once the signal light is emitted as stimulated radiation and exceeds absorption and spontaneous processes. In a three-level system,

$$N_1 + N_2 + N_3 = N_t \quad (3.6)$$

Combining the three light interaction rates and using the figure 3.2 above, the total population rate change in each state is given by,

$$\left(\frac{\partial N}{\partial t}\right) = \left(\frac{\partial N}{\partial t}\right)_{\text{Stimulated Absorption}} + \left(\frac{\partial N}{\partial t}\right)_{\text{Stimulated Emission}} + \left(\frac{\partial N}{\partial t}\right)_{\text{Spontaneous Emission}} \quad (3.7)$$

Therefore for state $|1\rangle$,

$$\begin{aligned} \frac{N_1(x, y, z, t)}{\partial t} &= \frac{I_p(x, y, z, t)}{h\nu_p} [\sigma_p^e(T)N_3(x, y, z, t) - \sigma_p^a(T)N_1(x, y, z, t)] + \dots \\ &\dots + \frac{I_s(x, y, z, t)}{h\nu_s} [\sigma_s^e(T)N_2(x, y, z, t) - \sigma_s^a(T)N_1(x, y, z, t)] + \dots \\ &\dots + \frac{N_2(x, y, z, t)}{\tau_{21}} \end{aligned} \quad (3.8)$$

State $|2\rangle$,

$$\begin{aligned} \frac{N_2(x, y, z, t)}{\partial t} &= \frac{N_3(x, y, z, t)}{\tau_{32}} - \frac{N_2(x, y, z, t)}{\tau_{21}} + \dots \\ &\dots + \frac{I_s(x, y, z, t)}{h\nu_s} [\sigma_s^e(T)N_2(x, y, z, t) - \sigma_s^a(T)N_1(x, y, z, t)] \end{aligned} \quad (3.9)$$

State $|3\rangle$,

$$\begin{aligned} \frac{N_3(x, y, z, t)}{\partial t} &= \frac{I_p(x, y, z, t)}{h\nu_p} [\sigma_p^e(T)N_3(x, y, z, t) - \sigma_p^a(T)N_1(x, y, z, t)] + \dots \\ &\dots - \frac{N_3(x, y, z, t)}{\tau_{32}} \end{aligned} \quad (3.10)$$

Laser Assumptions

In a real dynamic laser system, the doped atoms and population densities in the gain medium will vary in space and change with time $N_1(x, y, z, t)$, as well as the irradiance of the pump/signal light will vary with space and change with time $I(x, y, z, t)$. The cross section values are dependent on the spatial profile from a temperature T variation inside the gain medium that is caused from the previous two effects. To simplify the equations from complex phenomenon and mathematics, the following assumptions are made.

- Top-Hat Pump Laser – This assumption removes the spatial dependence of the irradiance profile. In a multi-mode fiber, the output beam does not follow a purely Gaussian beam since many modes are part of the output.
- Homogenous and Uniformly Doped Gain Medium – This assumption (with a top-hat pump), removes the spatial dependence of the population states.
- Constant Temperature Cross-Section – Since the thin disk uses a very thin gain medium and is heatsinked, it is assumed that the heat across the thin disk is uniform and is efficiently extracted out of the disk to maintain a constant temperature value.
- Steady-State Conditions – The laser is pumped with a CW pump source and after some time has passed, startup characteristics and time dynamic changes are removed, ultimately making the population rates,

$$\frac{\partial N_1}{\partial t} + \frac{\partial N_2}{\partial t} + \frac{\partial N_3}{\partial t} = 0 \quad (3.11)$$

- No Atoms in State $|3\rangle$ – In a three-level diagram, the spontaneous emission τ_{32} for Thulium is very fast compared to τ_{21} . Using equation (3.10), (3.11), and assumptions already stated, we obtain,

$$\frac{\partial N_3}{\partial t} = 0 = -\frac{N_3}{\tau_{32}} + \frac{I_p}{h\nu_p} (\sigma_p^a N_1 - \sigma_p^e N_3) \quad (3.12)$$

Therefore, with τ_{32} very small and solving for N_3 , we get,

$$N_3 = \frac{\sigma_p^a}{\sigma_p^e} \left[\frac{1}{1 + \frac{1}{\tau_{32} \sigma_p^e \left(\frac{I_p}{h\nu_p} \right)}} \right] N_1 = \frac{\sigma_p^a}{\sigma_p^e} \left[\frac{1}{1 + \infty} \right] N_1 = 0 \quad (3.13)$$

Since τ_{32} is very small, we conclude that N_3 is zero since the electrons in state $|3\rangle$ quickly relax to state $|2\rangle$. From this, we can assume the pumping process into state $|3\rangle$ can be part of state $|2\rangle$'s equations. This effectively removes the third state from the diagram and allows the system to be represented as a two-level diagram with the pumping process included.

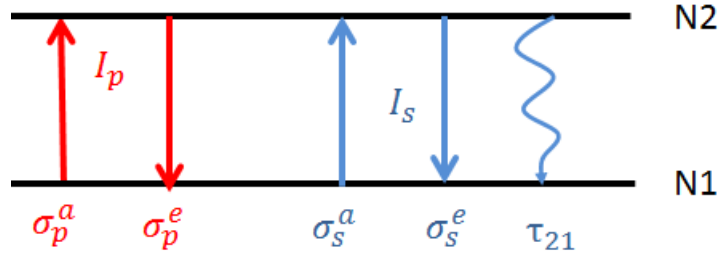


Figure 3.3 Simplified energy level diagram of Thulium.

3.3 Rate Equations

Population Rate Equations

Using the assumptions previously discussed, the population rate equations for Thulium are simplified to,

$$\frac{N_2}{\partial t} = 0 = \frac{I_p}{h\nu_p} [\sigma_p^a N_1 - \sigma_p^e N_2] + \frac{I_s}{h\nu_s} [\sigma_s^a N_1 - \sigma_s^e N_2] - \frac{N_2}{\tau_{21}} \quad (3.14)$$

$$\frac{N_2}{\partial t} = -\frac{N_1}{\partial t} \quad (3.15)$$

$$N_2 = N_t - N_1 \quad (3.16)$$

Combining equation 3.14 and 3.16 and solving for N_2 , the population in state $|2\rangle$ is,

$$N_2 = \frac{N_t \left[\frac{I_p}{h\nu_p} \sigma_p^a + \frac{I_s}{h\nu_s} \sigma_s^a \right]}{\frac{I_p}{h\nu_p} [\sigma_p^a + \sigma_p^e] + \frac{I_s}{h\nu_s} [\sigma_s^a + \sigma_s^e] + \frac{1}{\tau_{21}}} \quad (3.17)$$

which relates the population in state $|2\rangle$ based on the total amount of doped atoms in the gain media, as well as the pump power and signal power. Eventually, this will be used to calculate the signal output power.

Photon Rate Equations

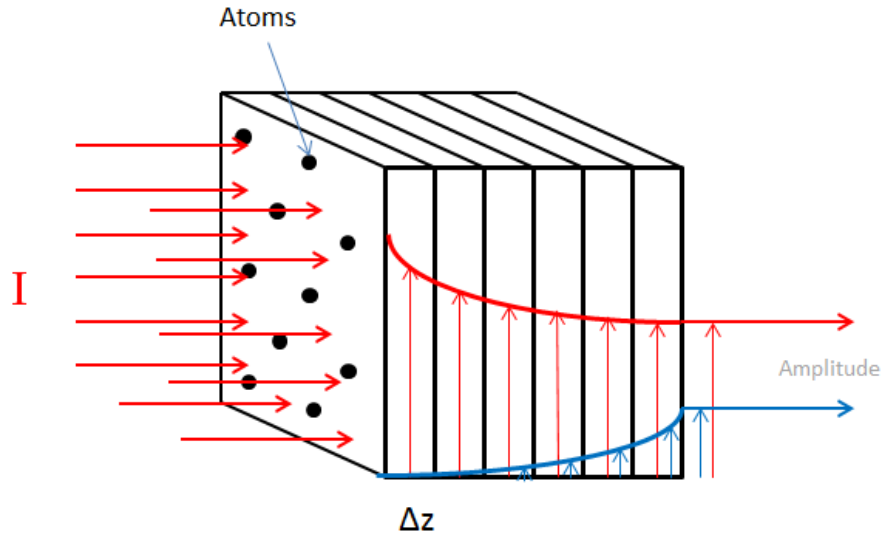


Figure 3.4 Gain and absorption of the gain material.

The pump light entering the gain medium is absorbed and the signal light is amplified. The gain and absorption of the material is given by,

$$\text{Pump Absorption} = \alpha = \frac{\partial I}{\partial z} = \sigma_p^e N_2 - \sigma_p^a N_1 \quad (3.18)$$

$$\text{Signal Gain} = g = \frac{\partial I}{\partial z} = \sigma_s^e N_2 - \sigma_s^a N_1 \quad (3.19)$$

Therefore, propagation through the gain media is,

$$I_p(z) = I_p0 * e^{-\alpha z} \quad (3.20)$$

$$I_s(z) = I_s0 * e^{g z} \quad (3.21)$$

3.4 Gain Threshold

The gain threshold equation describes the needed population density in the excited state $|2\rangle$ to exceed losses in the cavity so the signal can be amplified, which ultimately allows the laser to emit light. To trace the system, a linear cavity is used to derive subsequent calculations since the design (described in chapter 4), uses a linear cavity.

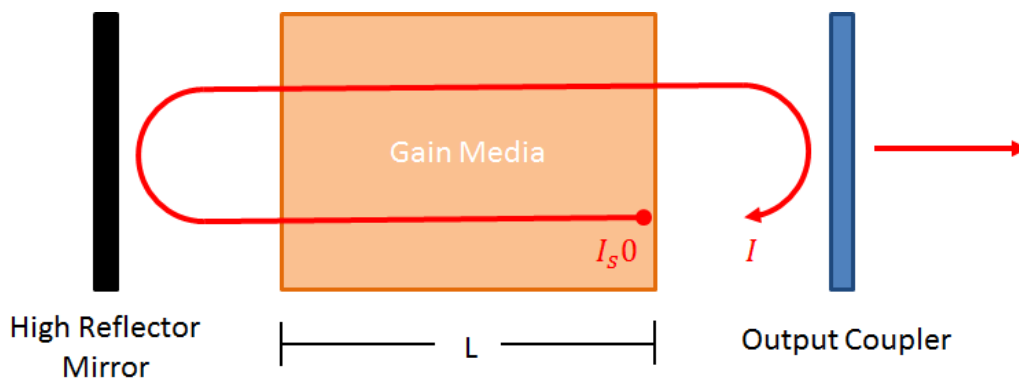


Figure 3.5 Linear cavity signal ray propagation for gain threshold.

Tracing a signal photon for a linear cavity, we see that the signal starts with an initial irradiance I_{s0} , and goes through the gain medium. Its intensity through the gain medium increases at a rate γ , over the distance L , with some energy being lost by scattering and other phenomenon l . The signal photon then reflects off the high reflecting mirror R_{HR} , and then enters the gain medium again. Lastly, the photon reflects off the Output Coupler R_{OC} , which ultimately completes the round trip. Any additional mirrors or loss mechanisms are factored in as another loss κ .

After 1 round trip of the photon, the following equation is formed,

$$I_s = I_{s0} \kappa R_{HR} R_{OC} e^{2(g-l)L} \quad (3.22)$$

For amplification of the signal to occur, $\frac{I_s}{I_{s0}}$ needs to equal 1. This gives the minimum parameters needed to maintain the signal after a round trip, which is called the resonator gain threshold g_{th} . Solving for g_{th} we obtain,

$$g_{th} > l + \frac{1}{2L} \ln \left(\frac{1}{\kappa R_{HR} R_{OC}} \right) \quad (3.23)$$

If the gain (3.19) is set equal to the resonator gain threshold (3.23), and by solving for N_2 , we calculate the minimum population $N_{2,th}$ so lasing can begin, which is defined by the equation,

$$N_{2,th} > \frac{l + \frac{1}{2L} \ln \left(\frac{1}{\kappa R_{HR} R_{OC}} \right) + \sigma_s^a N_t}{\sigma_s^e + \sigma_s^a} \quad (3.24)$$

3.5 Pump Chamber Power Contribution

As described earlier in section 2.3, the pump chamber combines a single laser source and overlaps the beam onto the thin disk by using 4 fold mirrors and a parabola. Tracing the pump ray is similar to the gain threshold equation trace.

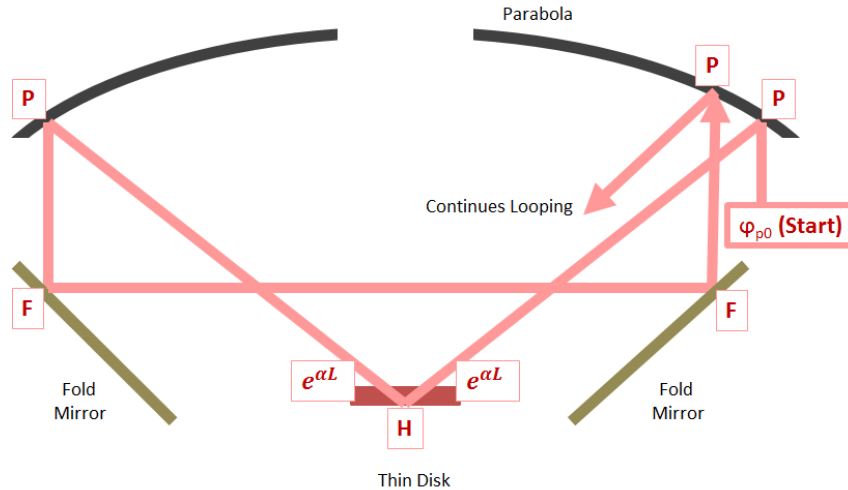


Figure 3.6 Associated pump power losses as the beam folds around the pump chamber.

The beam has an initial power ϕ_{p0} and reflects off the parabola with reflectance P . The light then focuses to the thin disk where the gain medium absorbs the light $e^{\alpha L}$, where L is the length of the gain material. The light then reflects off a high reflection coating R_{HR} on the backside of the thin disk to once again be absorbed $e^{\alpha L}$ in the gain medium. The light then continues to the parabola experiencing a reflection loss P again and reflection losses from the folding mirrors F . This continues looping around a number of times determined by the number of desired number of passes through the thin disk.

In this configuration, the pump experiences a ‘double pass’, since the light passes through the gain medium twice in nearly the same location. The total energy through the gain medium is assumed constant since the length L is very small, which makes the total pump energy nearly even throughout the length of the disk. The incident power through the thin disk is considered ‘forward’ light and the power after the thin disk is considered ‘backwards’ light.

Each beam's total power in the thin disk can be shown as,

$$\phi^{(t)} = \phi^{(f)} + \phi^{(b)} = \phi_0 + R_{HR}e^{2\beta L}\phi_0 \quad (3.25)$$

where ϕ_0 is the incident beam's power on the thin disk, R_{HR} is the reflection from the thin disk's high reflection coating, L is the thickness of the thin disk, and β is either the small signal absorption (α_0) coefficient or small signal gain (g_0) coefficient of the thin disk.

Considering only the pump p as the beam folds around the optics as in figure 3.6, each individual beam's total power through the thin disk after the first beam has passed is,

$$\phi_{pn}^{(t)} = P^2F^2R_{HR}e^{2\alpha L}\left(\phi_{p(n-1)}^{(f)}\right) + R_{HR}e^{2\alpha L}\left[P^2F^2R_{HR}e^{2\alpha L}\left(\phi_{p(n-1)}^{(f)}\right)\right] \quad (3.26)$$

where $\phi_{p(n-1)}^{(f)}$ is the previous beam's forward intensity. If all the beams are summed together, the total pump power through the thin disk is,

$$\phi_p = \phi_{p1}^{(t)} + \phi_{p2}^{(t)} + \dots + \phi_{pn}^{(t)} \quad (3.27)$$

Therefore, the single iterative equation for the total pump power through the thin disk is,

$$\Sigma\phi_p = P\phi_{p0} \sum_{n=1}^N (1 + R_{HR}e^{2\alpha L})(P^2F^2R_{HR}e^{2\alpha_0L})^{N-2n} \quad (3.28)$$

where N is the total number of passes through the thin disk. Equation 3.28 is also shown as a for-loop using MATLAB shown in appendix A.

3.6 Resonator Effects

As mentioned earlier in section 2.2.2, the laser output power decreases when the coupling efficiency between the signal and pump decreases. Therefore, an understanding of the resonator's effects on the system must be included in any model.

Signal Aperture Effect

According to Gaussian beam propagation, the spot size on the mirrors will increase as the resonator path length increases. This can be defined by,

$$w(z) = w_0 \sqrt{1 + \frac{z^2}{z_0^2}} \quad (3.29)$$

where $w(z)$ is the spot size at z , w_0 is the beam waist, z_0 is the Raleigh range, and z is the distance measured from the beam waist.

In the thin disk laser, the pump beam's spot size on the thin disk is essentially the limiting aperture in the system, shown in figure 3.7 below. Therefore, as the resonator length increases, the laser spot size overfills the pump spot size causing a decrease in pump-to-signal overlap. To account for such an effect, an equation relating the pump spot size to the laser beam spot size is needed.

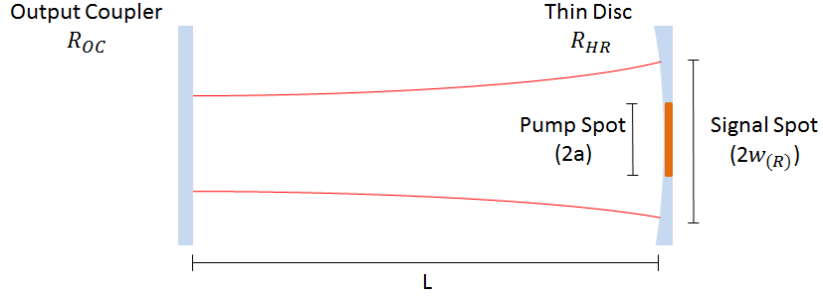


Figure 3.7 Aperture effect of pump focus in thin disk laser.

By relating the Fresnel number and the Gaussian beam radius to the area of the aperture [21]; we calculate the ratio of the aperture radius to the laser beam waist. Essentially, this is the ‘fill factor’ for the effective lasing spot size given by,

$$f_f = \frac{a}{w_{(R)}} = \pi \frac{p_r^2}{2Lg_2\lambda} \sqrt{1 - (2g_1g_2 - 1)^2} \quad (3.30)$$

where f_f is the fill factor, a is the aperture radius, $w_{(R)}$ is the beam radius at the mirror curvature, p_r is the pump spot size radius, L is the length of the resonator, and the g ’s are the “ g parameters” describing the stability of resonator with $g_{\#} = 1 - \frac{L}{r_{\#}}$ and $r_{\#}$ equaling the radius of the mirrors.

Pump-Signal Coupling Value

In any real laser system, misalignment of the resonator causes output power to decrease. The misalignment can be caused from mechanical sensitivity, thermal effects/distortions, or diffractive effects. To deal with such complex phenomenon, a simple factor will be included as part of the additional resonator losses κ shown in equation 3.22, and will be called κ_{sp} .

3.7 CW Power Output Model

Output Power Equations

If we set equal the gain threshold equation (3.24) and the population density equation 3.17, and then solve for I_s , we get the total signal irradiance inside the resonator $I_{s,res}$, which is given by,

$$I_{s,res} = \frac{\frac{I_p N_t}{h\nu_p} \sigma_p^a - \frac{I_p N_{2,th}}{h\nu_p} (\sigma_p^a + \sigma_p^e) - \frac{N_{2,th}}{\tau_{21}}}{\frac{N_{2,th}}{h\nu_s} (\sigma_s^a + \sigma_s^e) - \frac{N_t}{h\nu_s} \sigma_s^a} \quad (3.31)$$

with,

$$N_{2,th} = \frac{l + \frac{1}{2L} \ln\left(\frac{1}{\kappa_{sp} R_{HR} R_{OC}}\right) + \sigma_s^a N_t}{\sigma_s^e + \sigma_s^a}$$

and,

$$I_p = \frac{\Sigma\phi_p}{\pi(p_r/f_f)^2}$$

where $N_{2,th}$ is the population threshold, κ_{sp} is the signal-pump coupling efficiency value, $\Sigma\phi_p$ is the total pump power, p_r is the pump spot size radius, and f_f is the fill factor, all of which were defined in sections 3.3, 3.4, and 3.5.

Using equation 3.25 and 3.31, the backward signal power after the output coupler is defined as,

$$P_{s,out} = I_{s,res} \pi(p_r/f_f)^2 \frac{R_{HR} e^{2g_0 L}}{1 + R_{HR} e^{2g_0 L}} (1 - R_{OC}) \quad (3.32)$$

which gives the total power output for the thin disk laser system.

Yb:YAG Thin Disk Laser Comparison

To determine the accuracy of the model, measured data was used from a Dausinger-Guisen Yb:YAG laser module (TDM 1.0 Lab SMA). The following Yb:YAG parameter values were found from the vendor's datasheet.

Parameter	Symbol	Value
Signal Wavelength	λ_s	1030 nm
Pump Wavelength	λ_p	940 nm
Losses in Medium	l	0
Thickness of Thin Disk	L	220 μm
Diameter of Pump Spot	D_p	0.6 mm
Total Population Density	N_t	$7\% \times 1.38 \times 10^{20} \text{ cm}^{-3}$
Radiative Lifetime	t_{21}	967 μs
HR Thin Disk Reflectance	R_{HR}	99.5%
Output Coupler Reflectance	R_{OC}	98%
Parabolic Reflectance	P	99.5%
Fold Mirror Reflectance	F	99.5%
Number of Pump Beam Passes	N	24
Pump Absorption Cross Section	σ_p^a	$6.87898 \times 10^{-21} \text{ cm}^2$
Pump Emission Cross Section	σ_p^e	$1.52866 \times 10^{-22} \text{ cm}^2$
Signal Absorption Cross Section	σ_s^a	$1.22293 \times 10^{-21} \text{ cm}^2$
Signal Emission Cross Section	σ_s^e	$2.24204 \times 10^{-20} \text{ cm}^2$
Radius of Output Coupler	r_{OC}	∞ (Flat)
Radius of Thin Disk	r_{HR}	5600 mm
Length of the Resonator	L_{res}	100mm to 500mm
Signal-Power Coupling Efficiency	κ_{sp}	0.99*

Table 3.1 Dausinger-Guisen Yb:YAG system parameters for modelling.

Yb:YAG Model Comparison

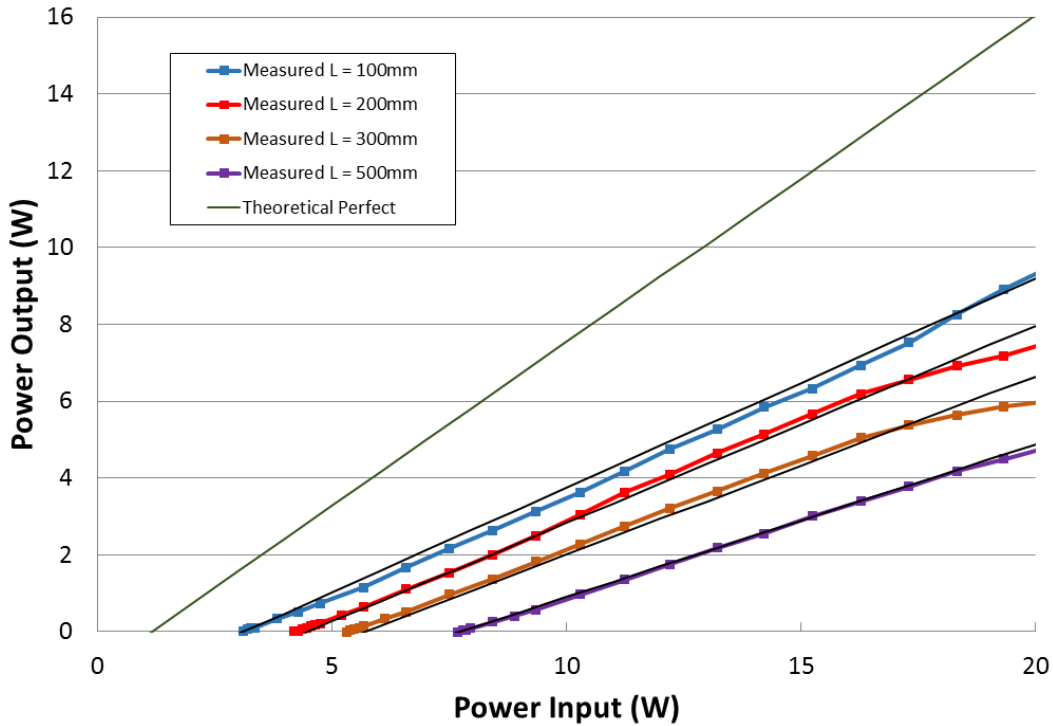


Figure 3.8 Power Output vs Power Input for theoretical and measured data of the Yb:YAG laser. L is the resonator length of the cavity. Black lines show the theoretical model for a particular κ_{sp} .

At first glance, the theoretical model compares very close to the measured data. This is enhanced since the signal-pump coupling values κ_{sp} were entered to match the slope of the experimental data. The reason for this was to develop an understanding of the misalignment tolerance caused in the laser system when the resonator length was increased, as well as to determine the accuracy of the laser threshold. If the slope efficiencies between theoretical and experimental values are far off, then the laser threshold comparison is not valid. However, if the signal-pump coupling values κ_{sp} are near 1 and match the experimental slope, then the model can be verified by comparing the laser threshold values.

Resonator Length	Slope Efficiency (Linear Regression of Experimental Data)	Signal-Pump Coupling Values (κ_{sp})
(@Perfect Overlap)	(0.853)	(1.000)
100 mm	0.546	0.9885
200 mm	0.519	0.9868
300 mm	0.465	0.9829
500 mm	0.398	0.9766

Table 3.2 Comparison of the slope efficiency and signal pump coupling values.

When comparing the signal-pump values shown in table 3.2, the values are all near 1 revealing that the alignment is good in the system. Also, it shows that small changes in the s-p coupling values κ_{sp} have a large effect on the slope efficiency of the laser. This reveals that the resonator is very sensitive to misalignments which can be caused by thermal effects and mechanical sensitivities.

Resonator Length	Measured Threshold	Theoretical Threshold	Difference
Perfect Overlap	-	0.944 W	-
100 mm	3.10 W	3.132 W	0.032 W
200 mm	4.19 W	4.481 W	0.291 W
300 mm	5.30 W	5.692 W	0.392 W
500 mm	7.69 W	7.735 W	0.045 W

Table 3.3 Model verification using threshold difference.

As can be seen in table 3.3, the laser threshold values compared very well. This shows that the model is accurate for predicting future design changes. It can be assumed that using an s-p coupling value κ_{sp} around 0.99 is a good starting point for predicting other laser's output power when the pump spot size is close to the laser spot size (fill factor ~ 1). In essence, the s-p coupling value κ_{sp} affects the slope efficiency of the laser, while the resonator length affects the laser threshold since the pump spot acts as an aperture (changes the fill factor f_f).

Chapter 4

Thin Disk Prototype Design

The goal of the prototype is to deliver a low cost Tm:Germanate thin disk laser, while providing the ability to test other gain material and learn about the characteristics of the thin disk architecture. Optical elements and mechanical supports were selected with heavy emphasis on using off-the-shelf items and available in-house materials.

To design the system, a three step iterative process was performed. Starting with first-order calculations, basic optical parameters were determined such as spot sizes, focal lengths, and beam dimensions. Next, optical elements were selected and the pump chamber was modeled using Non-Sequential ZEMAX for analysis and understanding of beam characteristics. Lastly, SOLIDWORKS was used to model the mechanics to determine physical locations and manufacturing capability. This was then re-iterated multiple times until a final design was selected.

4.1 Design Summary

Two parameters are arbitrarily selected for the thin disk architecture for which the optics and mechanics are all designed around.

1. Number of Passes Through Thin Disk – This determines the total pump power inside the gain medium. It is ideal to have as many passes as possible; unfortunately, this number is limited to 12 – 32 passes due to beam overlap, absorption of the pump, and supporting mechanics/optics.
2. Pump Spot Size – This determines the desired pump power density for laser threshold. To calculate the pump spot size diameter on the thin disk, we use the equation,

$$D_s = \frac{f_p}{f_c} D_f \quad (4.1)$$

where D_s is the pump spot size diameter, f_p is the parabolic focal length, f_c is the collimation optics focal length, and D_f is the diameter of the fiber.

First Order Summary

<u>Input</u>	<u>Value</u>
Fiber Core Diameter	105 μm
Fiber NA	.22
Number of Passes in Thin Disk	20
Space Between Spot Tolerance	± 1.7 mm
Collimation Optics Focal Length	10 mm
Parabolic Mirror Focal Length	35 mm
<u>Calculated</u>	<u>Value</u>
Collimated Beam Size	4.51 mm
Pump Spot Size Diameter	367.5 μm
Minimum Parabolic Mirror Diameter	68.52 mm

Table 4.1. Summary of first order Tm:Germanate design.

4.2 Component Selection and Manufacture

Pump Source

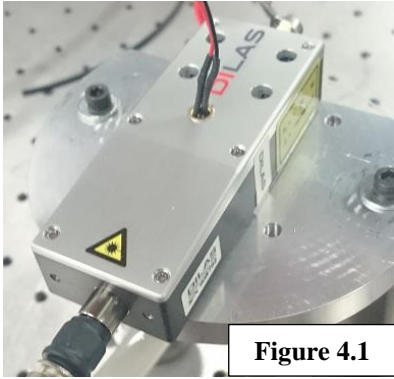


Figure 4.1

The selected source diode was a DILAS 793-105-1 fiber laser module. This uses a 105um fiber diameter with a NA of 0.22. Its emission has a FWHM of 2.6nm with a center peak at 793nm with a max output power of 32W. The diode was mounted on a water cooled plate using 100um

thick Indium layer to mate the diode to the surface.

Collimation Optics

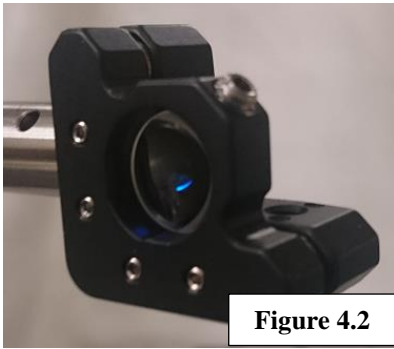
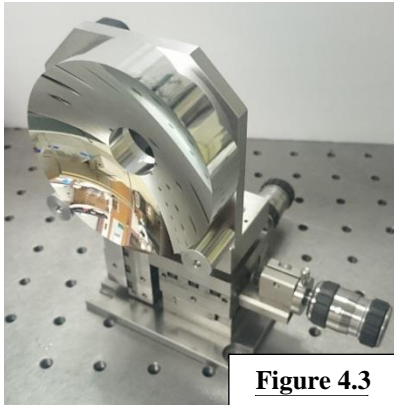


Figure 4.2

The collimating optic was selected as a single Thorlabs AL1210-B AR coated aspheric lens with a 10mm focal length. This optic was chosen due to no spherical aberration and a single lens mounting capability. The optic was mounted

using 5 points of alignment freedom (X, Y, Z, θ_x , θ_y) to give maximum adjustability.

Parabolic Mirror

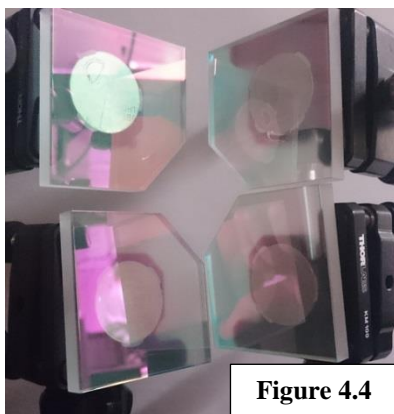


The focusing mirror was chosen to have a focal length of 35mm with an external diameter of 78mm and an internal hole aperture of 20mm. It was manufactured as a parabola (-1 conic constant) using an aluminum substrate with an enhanced aluminum coating centered at 795nm,

giving approximately a 95.5% reflection at 793nm. This mirror was selected due to its cheap cost and quick manufacturing time.

The parabolic mirror was mounted using a 5 point configuration with the radial supports at 90° separation for minimum radial deflection, and with three back supports equal spaced on a circle located at 0.707 of the radius for minimum axial deflection [22]. The mirror was then mounted using 5 points of alignment freedom (X, Y, Z, θ_x , θ_y) to give maximum adjustability.

Fold Mirrors



The four fold mirrors were selected using modified Thorlabs BBSQ2-E03 2"x2" square dielectric broadband coated mirrors (750-1100nm). They have a reflectance of $>99.5\%$ at 45° angle of incidence. The mirrors were modified using a diamond cutting wheel to cut

approximately a 1 inch angle off the corner of the mirror.

To mount the mirrors, aluminum blanks were created and bonded onto the back sides of the mirrors. Specifically, double sided sticky tape was mated between the aluminum blank and mirror, then three equal spaced tacks of UV adhesive (Optocast 3411) were applied to fixate the mirror to the aluminum. This was performed to minimize the stresses induced on the mirrors and to provide a very rigid bond between the aluminum and the glass mirror. The mirrors were then mounted in a fixture giving 4 points of alignment freedom (X , Z , θ_x , θ_y). In this mounting fixture, less than $1/10\lambda$ PV was achieved.

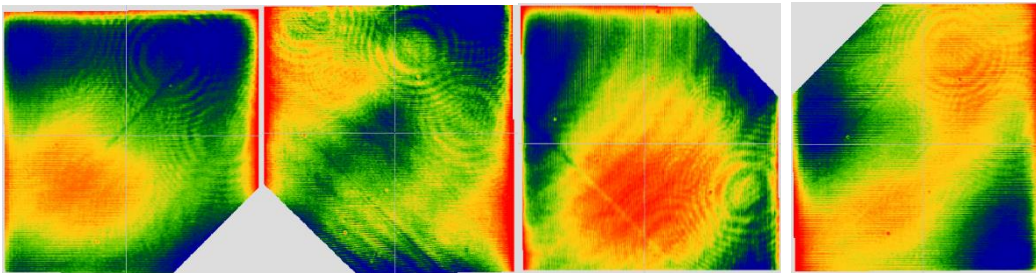
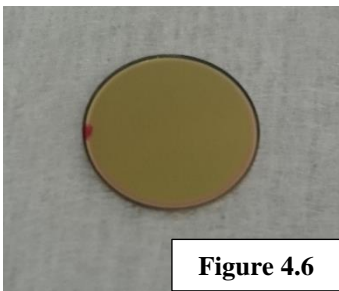


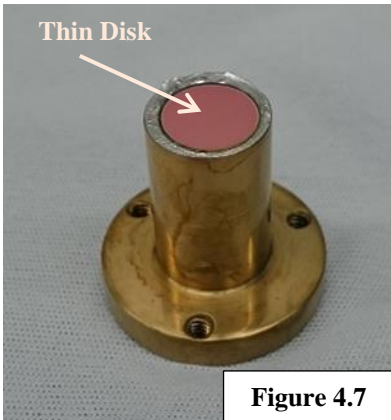
Figure 4.5 Interferometer measurements using a WYKO 6000.

Thin Disk

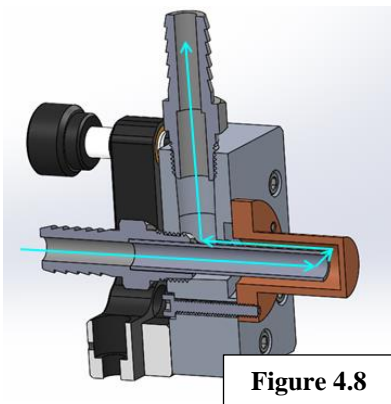


The thin disk gain medium was provided by NP Photonics using Thulium³⁺ with 2%wt doping in a Germanate glass matrix. The thin disk has dimensions of $\varnothing 10\text{mm} \times 250\mu\text{m}$ and has a broadband dielectric high transmission (HT) coating on one surface and a high reflection (HR) coating on the other. On the HR side, the thin disk was coated with a 100 μm Ti: Au layer for better adhesion of Indium. The thin disk itself is bonded onto a copper heatsink using an Indium thickness of $\sim 25\mu\text{m}$.

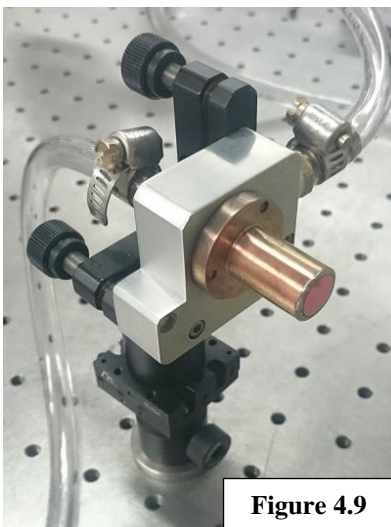
Thin Disk Heatsink



The heatsink uses a custom machined 99.9% copper mount with a wall thickness of $\sim 1\text{mm}$. The copper face was polished to a surface flatness about 0.95λ PV error. The copper heatsink was coated with $\sim 100\text{nm}$ Ti: Au to prevent oxidation and to prevent Indium from diffusing into it [27].



The design uses a water inlet to flow against the surface of the copper face where the thin disk is mounted. The tube in the center can be swapped out so water flowing into the thin disk surface can be optimized.



The thin disk heatsink was mounted using 3 degrees of alignment freedom (Z , θ_x , θ_y). The mechanical mounts were minimized to fit in the small working space available. The thin disk in the mount had less than a 1.1λ PV error.

Resonator Configuration

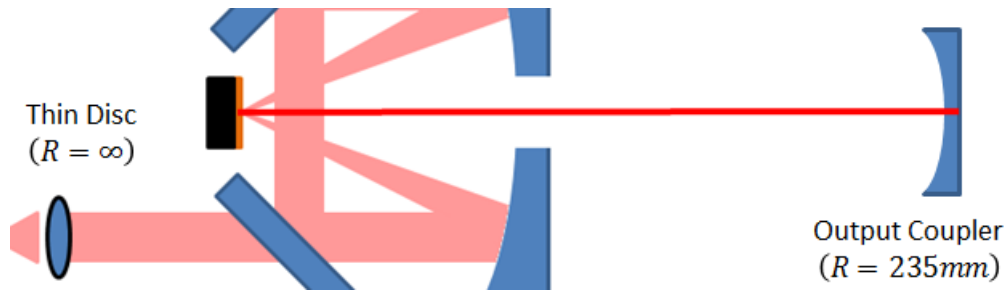


Figure 4.10 Tm:Germanate resonator configuration.

For the resonator design, a thin disk and an output coupler have already been provided. The thin disk is a flat optic ($R = \infty$) and the output coupler is a plano-concave 25.4mm diameter lens. The output coupler has a 250mm radius of curvature with a 98% reflective coating centered at 1910nm. For optimal results, the resonator design requires the use of a stable hemispherical resonator configuration using a linear cavity orientation.

To overlap the signal beam waist over the pump spot for optimal overlap ($f_f = 1$), the following equation for a stable hemispherical resonator is used to solve for the resonator length L ,

$$w_0^2 = p_r^2 = \frac{L\lambda}{\pi} \sqrt{\frac{g}{1-g}} \quad (4.2)$$

where w_0 is the beam waist, p_r is the pump spot radius, λ is the wavelength, L is the length of the resonator, and g is the “ g parameter” describing the stability of resonator with $g_{\#} = 1 - \frac{L}{R_{\#}}$.

Solving for L with the given components gives an optimal resonator length of 237mm.

Final System Layout

The optical system is laid out on a 12"x12" breadboard so the pump chamber can be transported for alignment and tested at different locations.

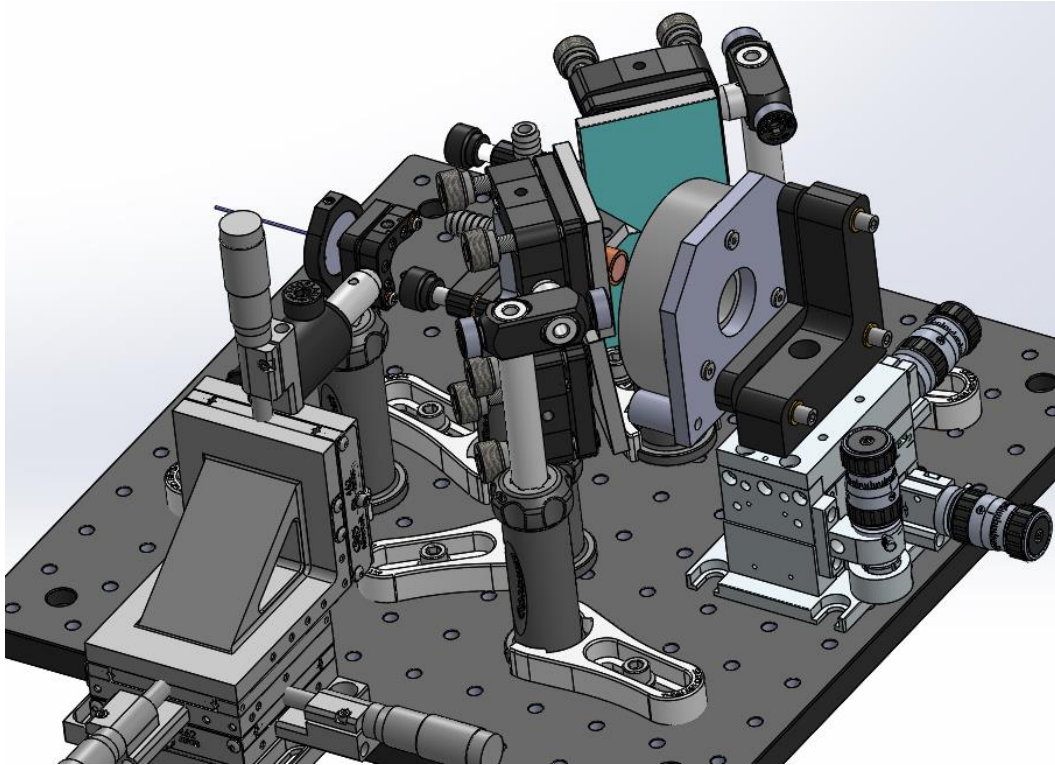


Figure 4.11 Solidworks model of pump module.

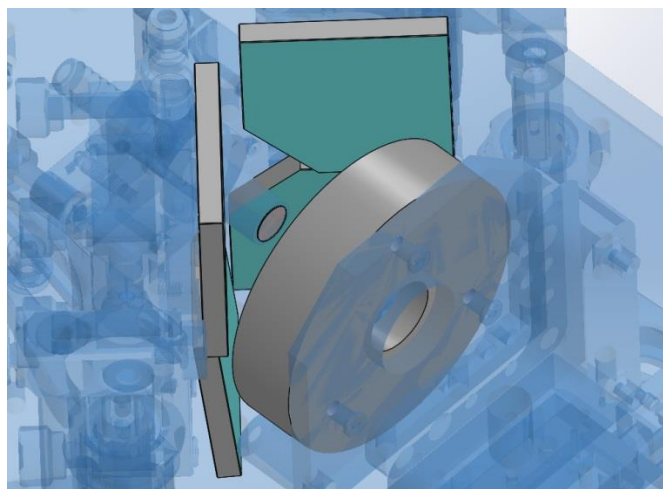


Figure 4.12 Solidworks model of pump optics.

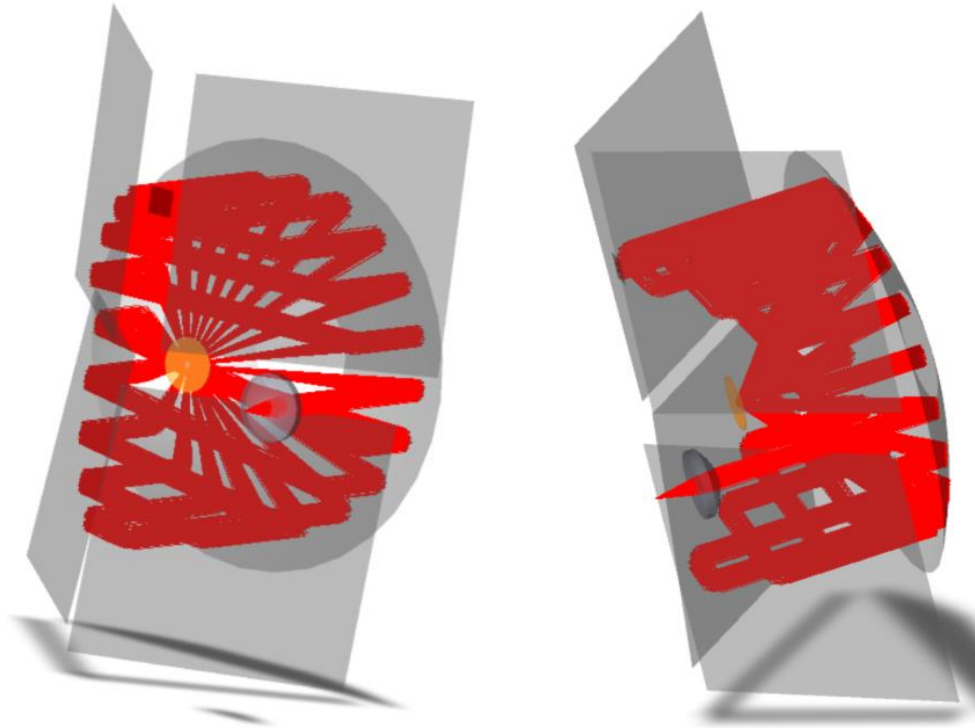


Figure 4.13 Non-Sequential Zemax layout of system (view 1 &2).

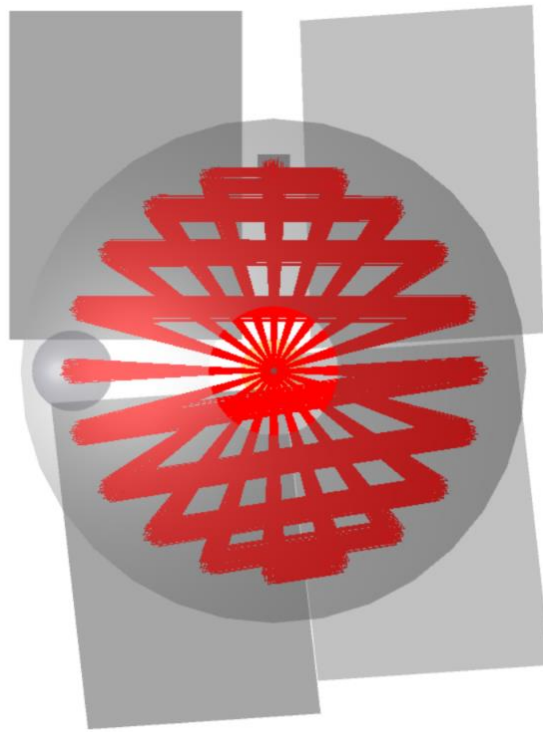


Figure 4.14 Non-Sequential Zemax beam path orientation (20 overlaps).

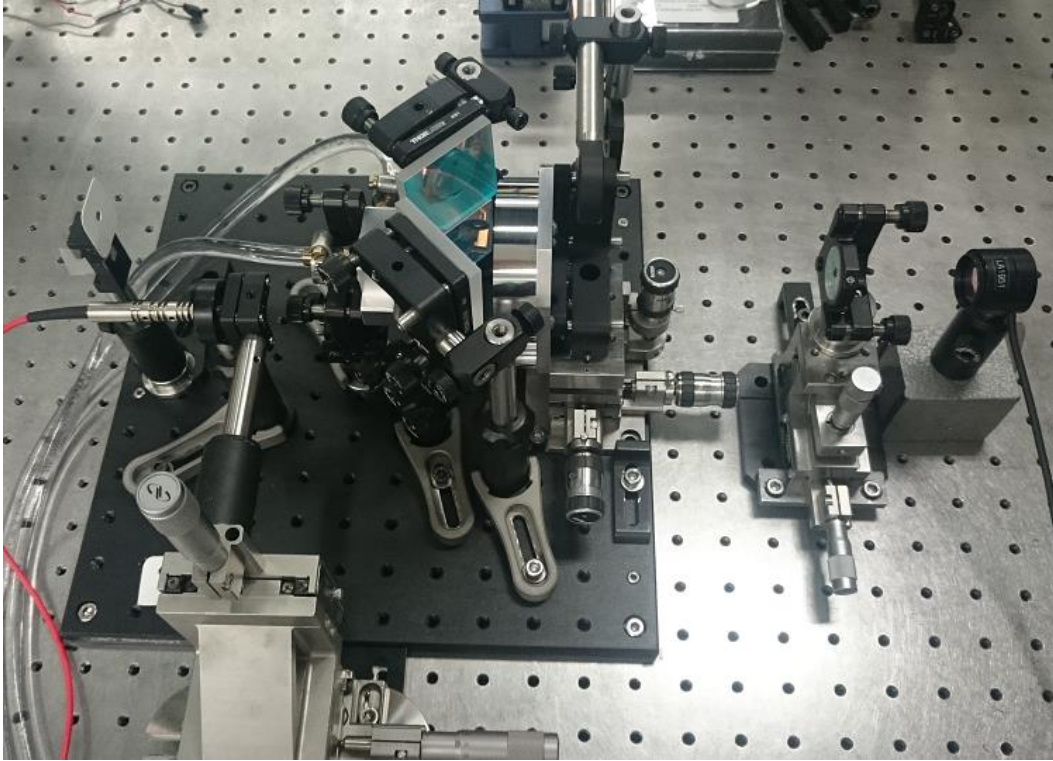


Figure 4.15 Real System layout.

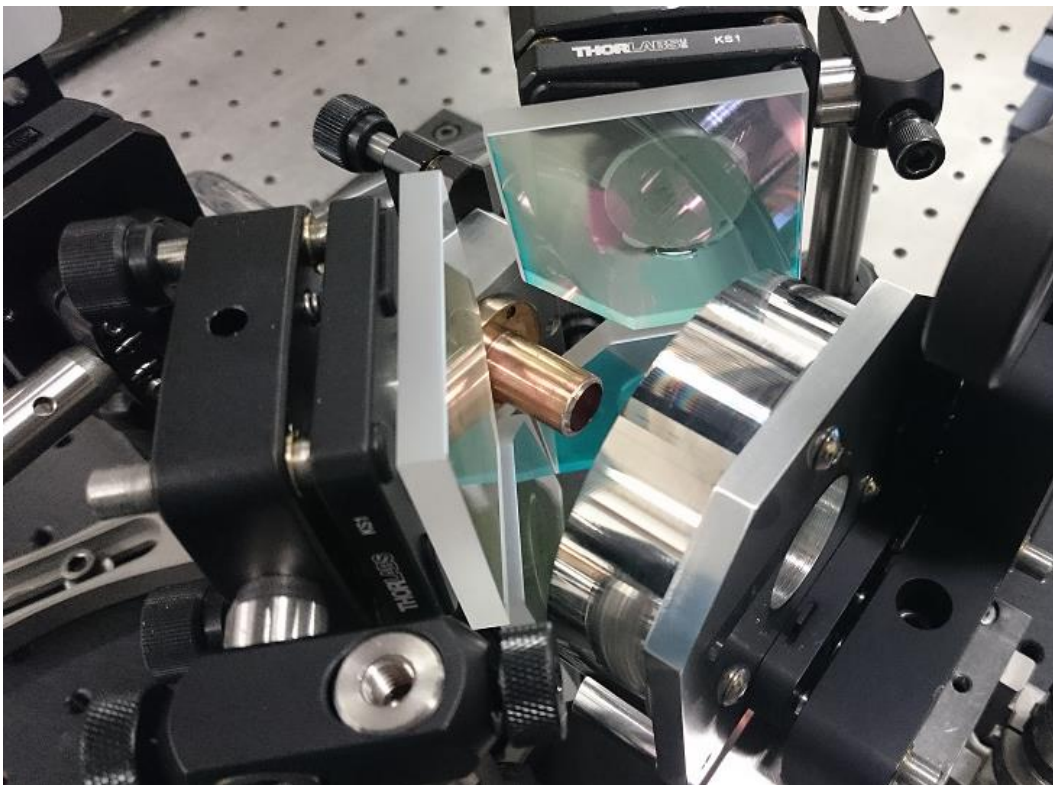


Figure 4.16 Pump optics layout (zoomed in).

4.3 Alignment and Assembly

The top-level process used to align the thin disk laser is presented. Actual step-by-step instructions for the pump chamber alignment are described in the appendix B. The process can incorporate other creative techniques and various devices/tools to ultimately achieve the same alignment goal. As a top level setup, the following alignment steps occurs,

- (i) Thin Disk Reference Mirror to Parabolic Mirror
- (ii) Four Fold Mirrors
- (iii) Pump Source and Collimation Optics
- (iv) Thin Disk and Resonator Optics

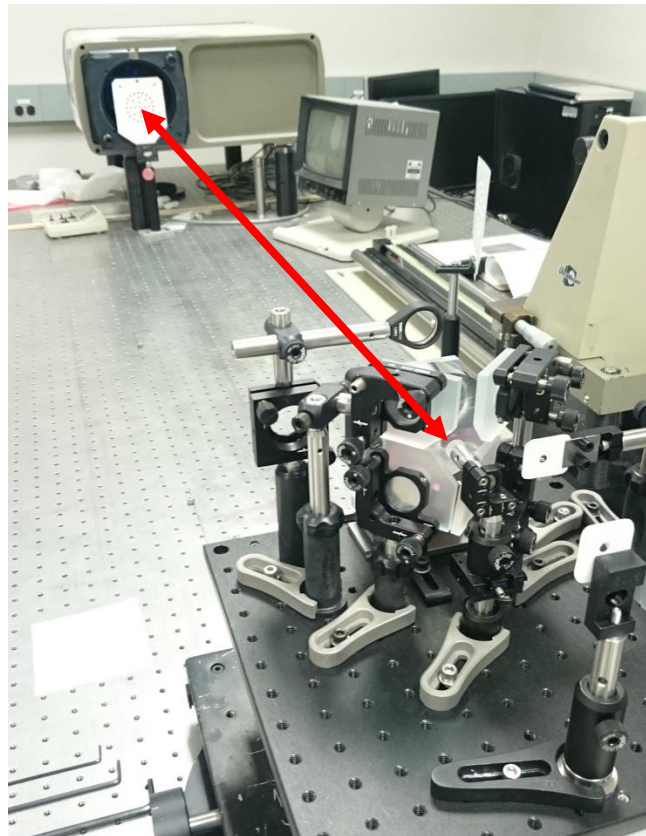


Figure 4.17 Pump chamber alignment using an interferometer as a large diameter collimator.

Thin Disk Reference Mirror to Parabolic Mirror

The parabolic mirror and the thin disk are the first critically aligned components. In the thin disk optical layout, the parabola collects collimated light from infinity and focuses it down to the thin disk. To align the thin disk components accurately, three main elements are used; (i) a collimated beam, (ii) a thin disk reference mirror, (iii) and a pinhole layout card.

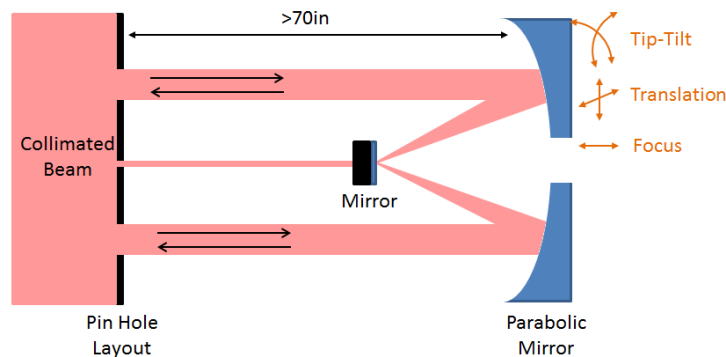


Figure 4.18 Parabolic mirror and thin disk alignment concept.

- (i) The collimator is used to project a highly accurate collimated beam to the parabolic mirror. This ensures the holes after the pinhole card are set in the exact same trajectory. Also, the diameter of the collimator needs to be greater than the diameter of the pinholes to ensure all beams spots are simulated. The distance to the parabola was very far (>70in) to ensure alignment was less than 0.25mRad accuracy.
- (ii) The reference mirror is used as a replacement for the thin disk during this initial process since the first surface reflection mirror makes it easier to see the beam and provides better reflections for alignment during future steps. Essentially, the thin disk reference mirror is aligned on-axis and retro-

reflected to the collimator. The thin disk can also be used, but the beam will be more difficult to see on the white retro-reflection pin-hole card.

- (iii) The pin-hole layout card is used to see the retro-reflections from the collimator after the mirror reflections. If the parabolic mirror to thin disk reference mirror is de-centered, tilted, or out of focus, the pinhole layout card will block the returned beams and will not project to the collimator. Each misalignment of the mirror has its own associated return beam pattern and characteristics. Also, the pinhole layout card has the same number of holes as the designed pump spot layout in the modeled system. This ensures the beam is able to fit into the clear apertures of the optics and that they are translated to the intended design.

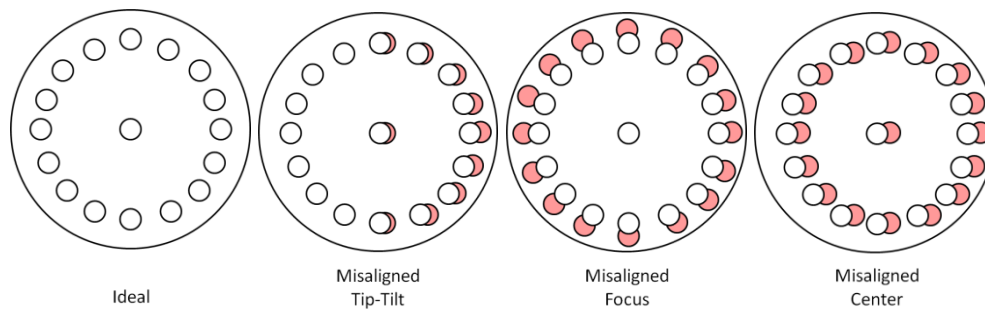


Figure 4.19 Pinhole misalignment characteristics for parabola to thin disk alignment.

Notice in figure 4.19, if translation is off, the spots will be evenly translated to one side. If there is tip-tilt between the mirrors, only a portion of the holes will retro-reflect through the holes, while the other half will not. And lastly, if the parabolic mirror is out of focus, the retro-reflected beams will be symmetrically misaligned around the pinholes.

Four Fold Mirrors

The four fold mirrors are the most critically aligned components in the entire setup. The mirror angles are dependent on the number of times the pump passes through the gain medium decided in the design. For this design, 20 passes of the thin disk was selected for two specific reasons; mechanical limitations of the mirror dimension to fit between two beams, and the clear aperture of the mirror's coating.

Only two critical components are needed to align the four fold mirrors; the auto-collimator, and a pin-hole layout card. Also, the parabolic mirror must be removed temporarily so the full layout of the beams can project to the four fold mirrors, and the setup must be spun around so the thin disk reference mirror faces the collimator. Removal of the parabolic mirror is supplemented by placing mechanical reference mounts so the parabola can be placed back into the system later with good enough accuracy.

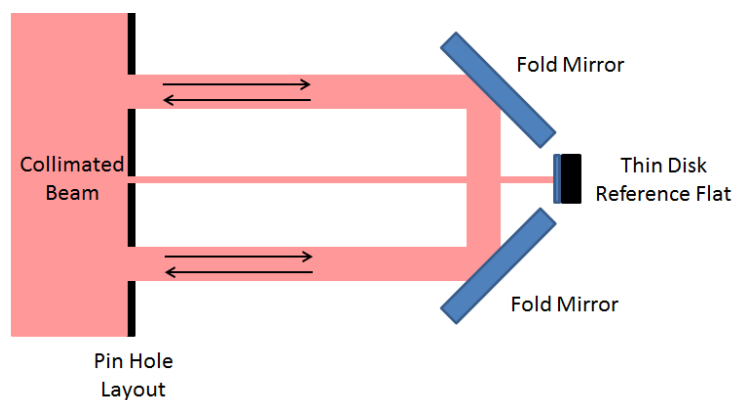


Figure 4.20 Thin disks four fold mirrors alignment concept.

The four fold mirrors are aligned to the auto-collimator by aligning the beams to pass through the pinhole card. The emphasis is to precisely position the necessary angles on the fold mirrors so that the beams coming in on-axis will leave on-axis in the correct locations. One of the pinhole beams that reflects off the thin disk alignment mirror needs to be centered in the same location as where the parabola focused its spots. This ensures the beam profile matches the parabola locations.

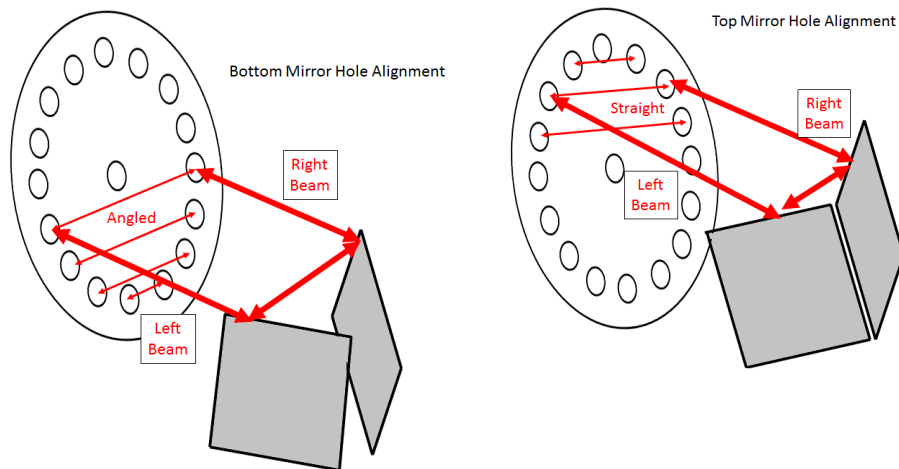


Figure 4.21 Angle adjustment of four fold mirrors.

In this setup, the bottom mirror angles are re-iteratively adjusted so that the beams go to the holes down or up from the opposite holes, depending on direction of travel (see figure 4.21, left). The top mirrors orient the beams symmetrically opposite of each other (figure 4.21, right). Mirrors are adjusted such that the left mirror needs to be adjusted to have the right beams go through the right holes, and the right mirror needs to be adjusted to have the left beam go through the left holes. This was re-iterated until all holes line up.

Pump Source and Collimation Optics

To align the pump source and collimation optics, the parabola needs to be placed back into the system at the mounting-hole locations from earlier. Adjustment of the parabolic mirror's focus allows the parabola to rely on mechanical tolerances for re-optimization. However, translation and tip-tilt of the parabola should be avoided since it will change the pump beam locations on the four fold mirrors and the beam may miss the clear aperture of the four fold mirrors.

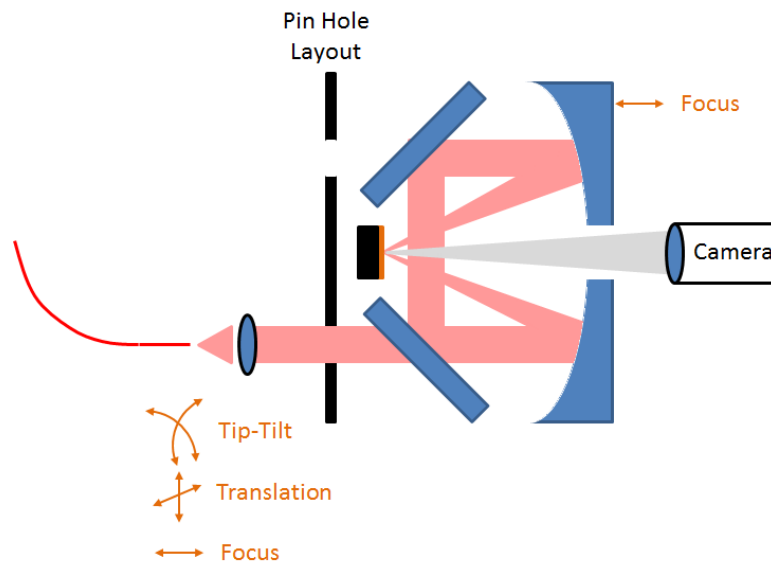


Figure 4.22 Source optics alignment concept.

In this setup, the fiber source and the collimation optics are tip-tilted to be on axis to the parabola, and they are also translated to go through the pinhole layout card positions. This ensures the beam will be at the same location as the design. Also, a camera was used to align the beams that are being focused by the parabolic mirror to ensure all spots overlap.

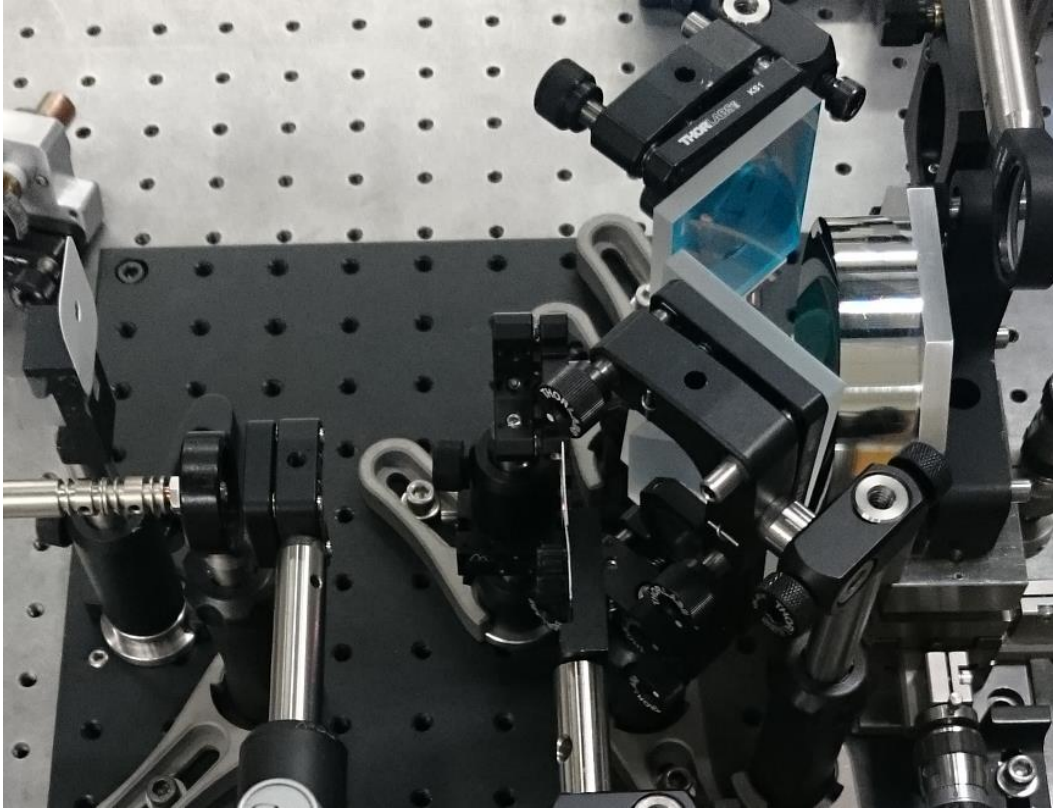


Figure 4.23 Prototype of source optics and pump chamber.

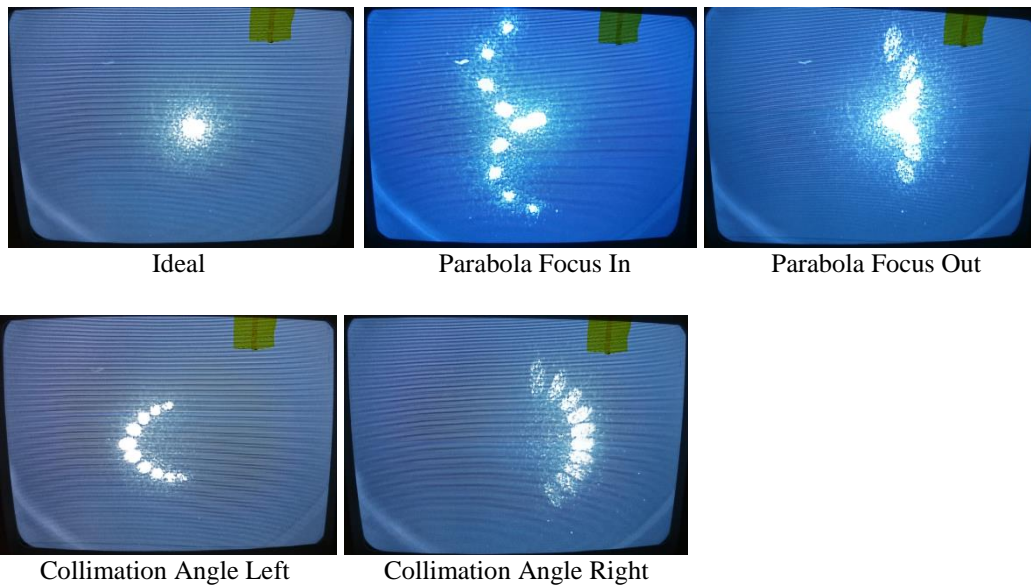


Figure 4.24 Source optics beam alignment characteristics.

Thin Disk and Resonator Optics

To align the thin disk or resonator, a pinhole card and a retro-reflection laser were needed. Three major portions to complete the alignment were,

- (i) Retro-reflection of the HeNe source over the pump spot on thin disk.
This sets the original alignment orientations of the thin disk.
- (ii) Replacement of the previous thin disk, and addition of the new thin disk gain medium. No other optics are adjusted other than the thin disk's tip-tilt (to retro-reflect HeNe source), and thin disk's Z-translation (to focus pump chamber).
- (iii) Alignment of resonator optic using retro-reflected beam and pin-hole card.

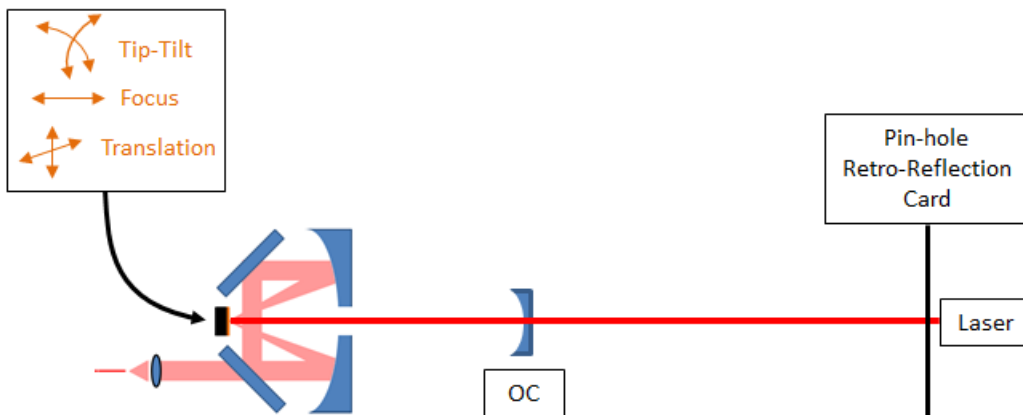


Figure 4.25 Resonator alignment concept.

Chapter 5

System Performance

To gain insight into the expected performance of the designed thin disk laser, several predictive models have been developed. The first model to understand is the pump chamber's optical performance and capabilities. The next presented model is the predicted power output with the selected components using the equations derived in chapter 3. Lastly, the experimental results of the system are presented and explained.

5.1 Pump Spot Analysis

To model the source and pump chamber, Non-Sequential ZEMAX was used. This gave detailed data on the beam characteristics and performance. The collected data from the input power was normalized to 1 Watt to give insight into intensity variations. Resonator pulse propagation and beam quality have not been analyzed in this thesis since we are only concerned with the power output.

Fiber Source

The pump source was first characterized and modelled to accurately analyze the final pump spot onto the thin disk. Capturing the beam profile consisted of measuring the output of the DILAS 793nm fiber diode by scanning across horizontally with a power meter using a small pinhole aperture. The data was then compiled, normalized, and divided into 10 segments. This data was then entered into ZEMAX; specifically, the source was modelled using a ‘Radial Source’ object type with the data from the 10 segments calculated earlier, as well as the fiber emission angle calculated from the NA given from the DILAS fiber datasheet.

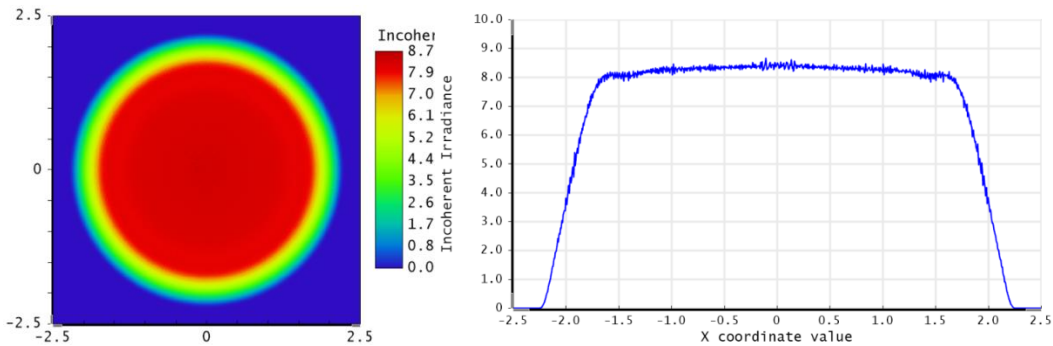


Figure 5.1 Zemax modelled data from a DILAS 793nm fiber diode.

As can be seen in the horizontal profile, the beam width after the collimating lens (at the $\frac{1}{e^2}$ radial location point), compares very close to the first order calculated value of 4.51mm. This should give a good indication how the pump spot looks like in the thin disk.

Pump Spot

With an accurate input source model shown previously, the effects from the pump chamber can be accurately modelled. Reflection losses (gathered from vendor datasheets) have been modelled in the system as well, but absorption in the gain has not. To account for this, an increased reflection loss was added to the HT side of the thin disk to represent the absorption loss since the intensity has a double pass of the pump light. To analyze the results, a detector face was placed 0.00001mm in front of the HR surface, as well as a detector face 0.00001mm in front of the HT face. This was used to help evaluate the total irradiance passing as a double pass through those locations.

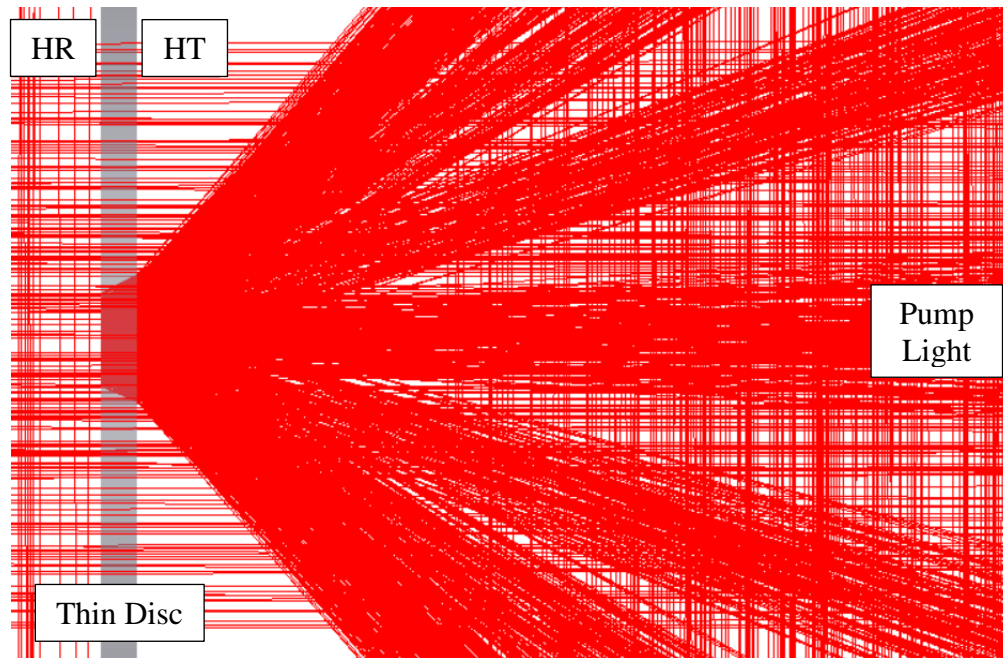


Figure 5.2 Pump spot's cross section at the thin disk focus.

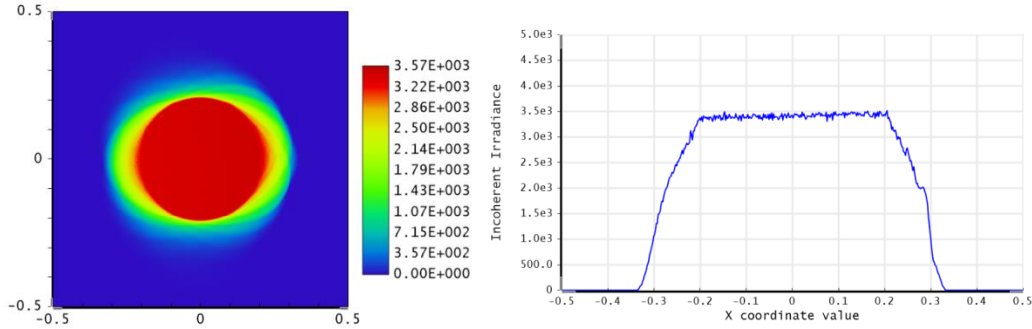


Figure 5.3 Pump spot on thin disk HR side (zoomed in).

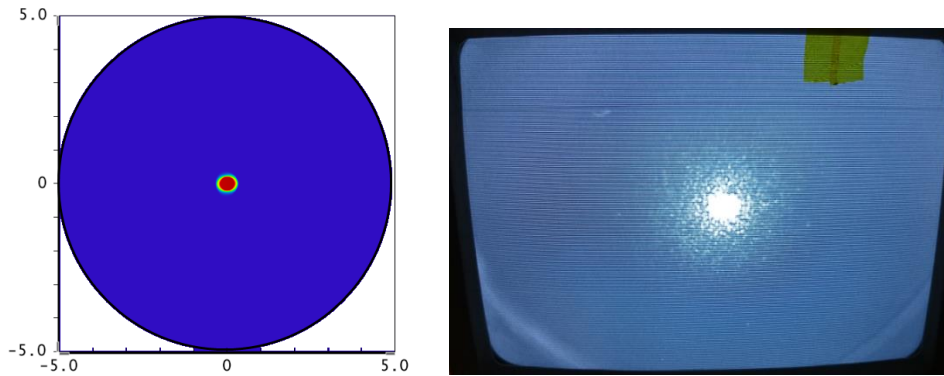


Figure 5.4 Comparison of pump spot on thin disk HR side.

The model shows a spot size very close to the first order calculated value of 367.5um width. The beam shows an elliptical pattern due to the astigmatism created by the thin disk, as well as the first pass through of the thin disk having the highest intensity. It is safe to assume a top hat pumping scheme for modeling purposes shown in chapter 3.

When all beams were overlapped in the final system, the beam size was measured to be approximately 400um. This was due to aberrations and misalignment. Overall, the system is considered well aligned to theoretical expectations.

Tm:Germanate Output Power Model

Using the model derived in chapter 3, the output power is calculated for the components selected in chapter 4. The table below shows the constants used for the model.

Parameter	Symbol	Value
Signal Wavelength	λ_s	1910 nm
Pump Wavelength	λ_p	793 nm
Losses in Medium	l	0
Thickness of Thin Disk	L	250 μm
Diameter of Pump Spot	D_p	367.5 μm
Total Population Density	N_t	$5.2 \times 10^{26} \text{ m}^{-3}$
Radiative Lifetime	t_{21}	$2.5 \times 10^{-3} \text{ sec}$
HR Thin Disk Reflectance	R_{OC}	99.5%
Output Coupler Reflectance	R_{HR}	98%
Parabolic Reflectance	P	95.5%
Fold Mirror Reflectance	F	99.5%
Number of Pump Beam Passes	N	20
Pump Absorption Cross Section	σ_p^a	$4.472800 \times 10^{-25} \text{ m}^2$
Pump Emission Cross Section	σ_p^e	$1 \times 10^{-100} \text{ m}^2$ (No Info)
Signal Absorption Cross Section	σ_s^a	$0.129504 \times 10^{-25} \text{ m}^2$
Signal Emission Cross Section	σ_s^e	$1.8114100 \times 10^{-25} \text{ m}^2$
Radius of Thin Disk	r_{HR}	∞ (Flat)
Radius of Output Coupler	r_{OC}	250 mm
Length of the Resonator	L_{res}	237 mm
Signal-Power Coupling Efficiency	κ_{sp}	~.99* (Varying)

Table 5.1 Tm:Germanate model parameters.

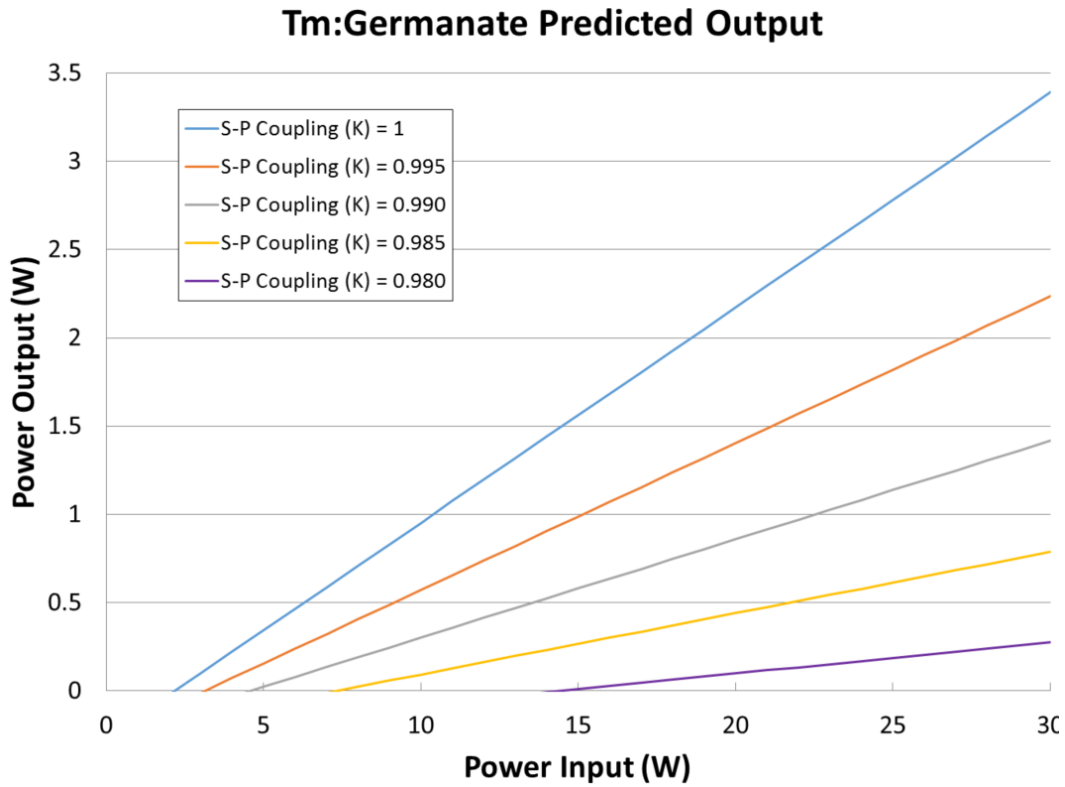


Figure 5.5 Tm:Germanate power output vs power input for various s-p coupling values κ_{sp} .

S-P Coupling κ_{sp} Value	Threshold	Slope Efficiency
1	2.189	12.2%
0.995	3.127	8.3%
0.990	4.592	5.6%
0.985	7.299	3.5%
0.980	14.336	1.8%

Table 5.2 Threshold and slope efficiency values for various s-p coupling values.

As can be seen in table 7, the laser is potentially operable with the given components, but is very sensitive to the signal-pump coupling values. Meaning, the laser system is expected to be very sensitive to misalignment.

Experimental Results and Conclusion

Unfortunately, the system was unable to lase. As shown earlier in the predicted model output, the laser is very sensitive to misalignment. Ultimately though, the issue relates to the transfer of heat from the thin disk to the copper heatsink. When the thin disk was pumped with light, the disk warped causing the system to be completely misaligned. In fact, when the resonator was pumped with a meager 2 watts of input power, the thin disk spot temperature was over 140°C. The temperature warpage caused the pump beam in the chamber to diverge after the first pass making the gain medium only experience 2 passes rather than the 20 passes as originally designed. This decreased the efficiency, which then required more input energy to reach lasing threshold, and therefore more distortion effects. Bottom line, the resonator cannot be aligned with the thermal limitation experienced from the thin disk.



Figure 5.6 Pump spot temperature experience in thin disk.

As can be seen in the figure above 5.6, the temperature on the thin disk is not extracted out efficiently. Damage occurs at approximately 500° C, which is the approximate glass transition point of Germanate [20]. The heat dynamic inside the glass is unknown; however, multiple thermal compounds and mating

techniques have been performed to mate the thin disk to the copper heatsink, but all failed. Indium, Antec Formula 7 Nano-Diamond thermal compound, and Artic Silver Alumina ceramic compound, were all unsuccessful in transferring the heat better. Using a chopper to pulse the laser did help by lowering the temperature on the thin disk by nearly half. Unfortunately, the temperature experienced in the thin disk is still exceeding 170°C at only 6W input power.

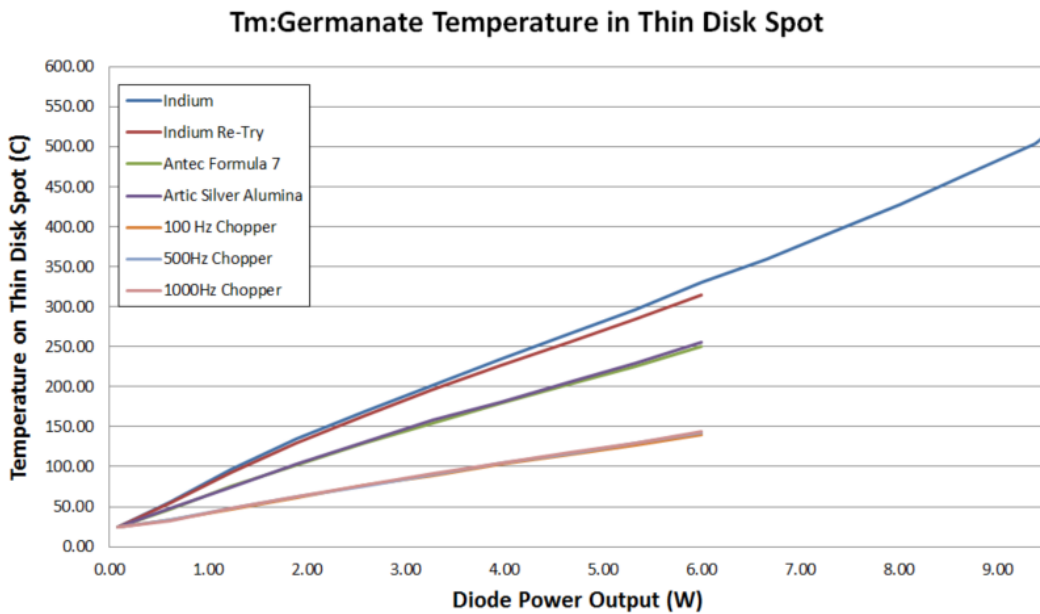


Figure 5.7 Tm:Germanate thin disk temperature vs power input for various interface materials.

Comparing the system to the Dausinger-Guisen Yb:YAG pump module shown in figure 5.8 below, the temperature on the thin disk is magnitudes below at equivalent input powers. For instance, at a disk input pump power $\sim 25\text{W}$, the temperature on the Yb:YAG thin disk was only 40°C .

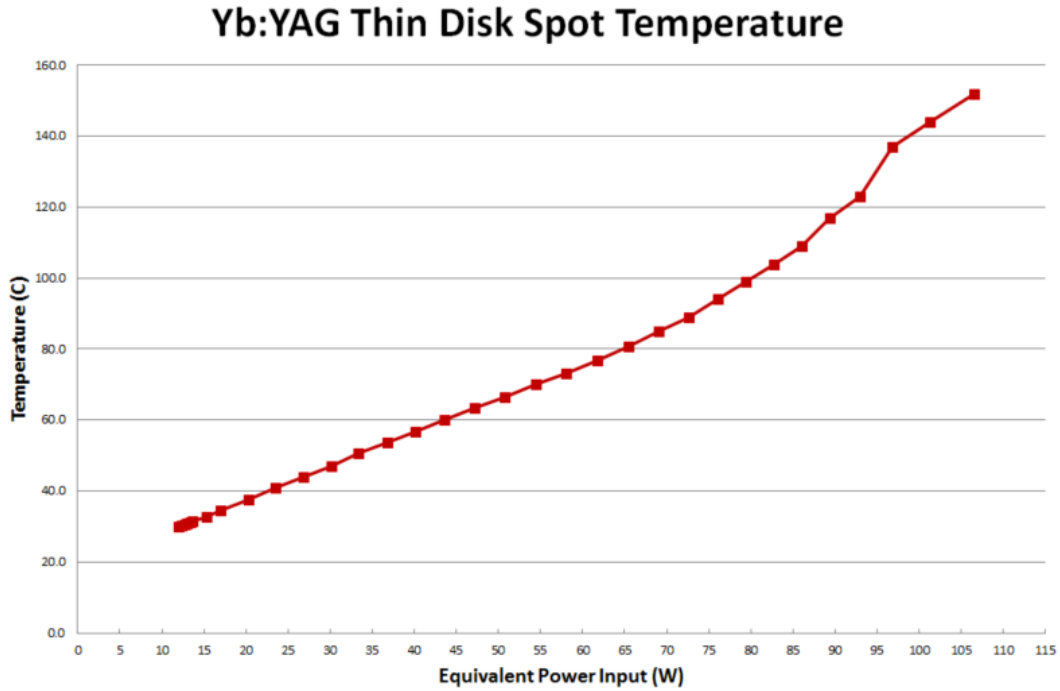


Figure 5.8 Pump spot temperature in Yb:YAG thin disk laser.

In conclusion, the Tm:Germanate laser will not lase unless the thin disk's heat is extracted out. Even though the thin disk will not lase, detailed design instructions, models, and alignment processes have been developed so other gain materials and enhancements to the thin disk can be experimented with.

Appendix A – MATLAB Model Code for Tm:Germanate

```

%Power Output Calculation Chapter 3
%Tm:Germanate (Current Configuration)

close all;
clc
clear all;
format long;

%Laser Design Parameters
p_wavelength = 793*10^(-9);
s_wavelength = 1910*10^(-9); %Laser Signal Wavelength(m)
loss = 0; %Loss due to scattering, etc...
gain_thickness = 250e-6; %Thin disk thickness (m)
p_spotsize = 367.5e-6; %Pump Spot Size (m)
Nt = 5.2e26; %Doping Concentration of Glass (1/m^3)
t21 = 2.5e-3; %Spontaneous Emission Coefficient (s)
HR_reflect = .9995; %Reflectivity of Mirror 1 (HR Mirror)
OC_reflect = 0.98; %Reflectivity of Mirror 2 (OC Mirror)
num_p_spots = 20; %Number of Thin Disk Passes
mirrors_reflect = .995; %Reflection of 4 Fold Mirrors
parabola_reflect = .955; %Reflection of Parabolic Mirror
T = 300; %Temperature of Thin Disk
R1 = 1e100; %Radius of Curvature of Flat Mirror
R2 = .250; %Radius of Curvature of Curved Mirror
L_res = .237; %Length of the Resonator
sp_coupling = 1; %Signal-pump Coupling Efficiency Value

%Resonator Parameters
g1 = 1 - L_res/R1;
g2 = 1 - L_res/R2;
%Beam Radius for Hemispherical Configuration
wFM = sqrt((L_res*s_wavelength/pi)*sqrt(g2/(1-g2)));
%Beam Diameter for Hemispherical Configuration
wCM = sqrt((L_res*s_wavelength/pi)*sqrt(1/(g2*(1-g2))));
D_FM = 2*wFM*1e3; %Spotsize on Flat Mirror (mm)
D_CM = 2*wCM*1e3; %Spotsize on Curved Mirror (mm)
G = 2*g1*g2-1;
N = (p_spotsize/2)^2/(2*L_res*g2*s_wavelength);
fill_factor = (pi*N*sqrt(1-G^2))^(.5);
spotsize = p_spotsize/fill_factor; %Pump Spot Size (m)
%Area of the Pump Spot Size (or Core) (m^2)
A_spotsize = (pi * spotsize.^2 / 4);

%Graphing Parameters
Pp0 = 1e-100:1:35; %Pump Power

%Initial Parameters/Constants
h = 6.62607*10^(-34); %Planks Constant (m^2*kg/s);
c = 2.99792458*10^8; %Speed of Light (m/s)

%Other Parameters
v_s = c / s_wavelength; %Signal Frequency
v_p = c / p_wavelength; %Pump Frequency;

```

```

%Cross Section
p_cross_a = .4472800e-24;
p_cross_e = 1e-100;
s_cross_a = .0129504e-24;
s_cross_e = .18114100e-24;

%Pump Factor Increase
N2_th = (loss +
(1/(2*gain_thickness))*log(1/(sp_coupling*OC_reflect*HR_reflect))
+s_cross_a*Nt)/(s_cross_e+s_cross_a);
a0 = p_cross_e*N2_th-p_cross_a*(Nt-N2_th);
g0 = s_cross_e*N2_th-s_cross_a*(Nt-N2_th);

%Derived Solution
for i = 1:length(Pp0)

    %Calculate Total Pump Irradiance Through Thin Disk
    Pp = 0;
    Pp_temp = Pp0(i); %Pump Power
    for j = 1:num_p_spots/2
        %Reflection off Parabola
        Pp_temp = Pp_temp*parabola_reflect;
        Pp = Pp + Pp_temp; %Double Pass Addition
        %Loss Through Thin Disk
        Pp_temp = Pp_temp*exp(a0*gain_thickness);
        %Reflect off Thin Disk HR Side
        Pp_temp = Pp_temp*HR_reflect;
        %Loss Through Thin Disk
        Pp_temp = Pp_temp*exp(a0*gain_thickness);
        %Addition of Pump Into Second Pass of Thin Disk
        Pp = Pp + Pp_temp; %Double Pass Addition
        %Reflect off Parabola
        Pp_temp = Pp_temp*parabola_reflect;
        %Reflection Loss Off Mirrors
        Pp_temp = Pp_temp*mirrors_reflect.^2;
    end
    p_factor = (Pp)/Pp0(i);%For my own analysis

    Ip = Pp/A_spotsize;
    Is_res = (((Ip*Nt)/(h*v_p))*p_cross_a-
((Ip*N2_th)/(h*v_p))*(p_cross_a+p_cross_e)-
N2_th/t21)/(((N2_th)/(h*v_s))*(s_cross_a+s_cross_e)-
((Nt)/(h*v_s))*s_cross_a);

    Ps_res = Is_res*A_spotsize;
    Ps_backward =
Ps_res*((HR_reflect*exp(2*g0*gain_thickness))/(1+HR_reflect*exp(2
*g0*gain_thickness)));
    Ps_out(i) = (1-OC_reflect)*Ps_backward;

end

Pp_th = (N2_th*h*v_p)/(t21*(Nt*p_cross_a-
N2_th*(p_cross_a+p_cross_e)))*(A_spotsize)/(p_factor);
fprintf('Threshold Value = %s\n', num2str(Pp_th,'%3f'));
fprintf('Slope Efficiency = %s\n', num2str(100*(Ps_out(18)-
Ps_out(16))/(Pp0(18)-Pp0(16)),'%1f'));

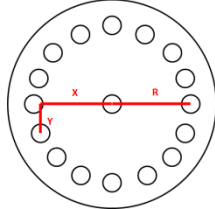
```

```
figure;
plot(Pp0, Ps_out);
title('Laser Out vs Fiber Input'); xlabel('Fiber Input Power
(W)'); ylabel('Is Out (W)');
%axis([0, length(Ip0), 0, 60]);

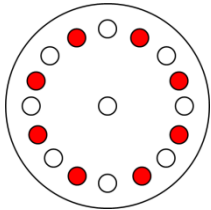
%Save File
final_result=[Pp0',Ps_out'];
save 'TDL_MyDerived_Model_Tm-Germanate.txt' final_result -ASCII;
```

Appendix B – ZEMAX Pump Design Procedure

1. Determine the number of passes through the thin disk and calculate the cross angle distances.



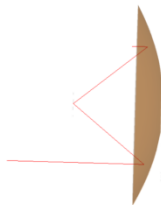
2. Load Non-Sequential Zemax and set the wavelength and parameters.
3. Add in 8 surfaces and make them symmetrically placed around a surface at the desired radial distances with diameters equal to the beam spot size calculated by first order parameters.
 - Change surface transparencies to 40%.
 - Select 'Always' for the option 'Rays Ignore Object'.



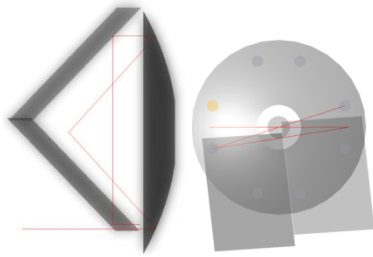
4. Add in a parabolic mirror and a flat mirror as a 'standard surface'.
 - Place the flat mirror at the focal point of the parabola.
 - Change optic transparencies to 40%.



5. Insert a "Source Ray" and project the ray at the radial distance desired into the parabola.



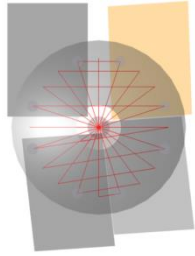
6. Add in 2 mirrors 'Rectangle' to the bottom and optimize angles of 2 bottom fold mirrors by optimizing the exiting ray.
 - Start with 45° tilt about Y for the mirrors.
 - Manually adjust the mirrors X, Y, and Z positions such that the surfaces created in step 3 are in the clear aperture of the mirrors. Only bottom right Z position needs to be fixed precise for desired distances away from the parabolic mirror.
 - Place variables on X and Y tilt, as well as bottom left mirror Z Position.
 - Ensure to set the correct segment number when optimizing in merit function. You should use the segment of the propagating ray into the parabolic mirror after the first reflection off the thin disk mirror. Also ensure crossing beam's reflections are perpendicular to optical axis.



Object Type	Comment	X Position	Y Position	Z Position	Tilt About X	Tilt About Y	Tilt About Z	Material	# Layout Rays	# Analysis Rays
1 Source Ray	Alignment Ray	-31.00000	0.00000	-60.00000	0.00000	0.00000	0.00000		1	0
2 Standard Surface	Parabolic Mirror	0.00000	0.00000	0.00000	0.00000	0.00000	0.00000	MIRROR	-70.00000	-1.00000
3 Standard Surface	Thin Disk Mirror	0.00000	0.00000	-35.00000	0.00000	0.00000	0.00000	MIRROR	0.00000	0.00000
4 Rectangle	Mirror 1	22.00000	-21.50000	-33.00000	8.89098 V	-44.29887 V	9.00000	MIRROR	25.40000	25.40000
5 Rectangle	Mirror 2	-13.50000	-29.00000	-33.49541 V	-8.89098 P	44.29887	9.00000	MIRROR	25.40000	25.40000

Type	Surf	Src#	Splt?	Pol?	Seg#	Data	Source #	Target	Weight	Value	% Contrib
1 NSRA	1	1	0	0	6	4	1	-1.00000	1.00000	-0.98769	99.99935
2 NSRA	1	1	0	0	6	1	1	-29.48275	1.00000	-29.48275	1.59697E-005
3 NSRA	1	1	0	0	6	2	1	-9.57953	1.00000	-9.57950	6.36613E-004
4 NSRA	1	1	0	0	-1	4	1	0.00000	1.00000	-4.23796E-009	1.18491E-011
5 NSRA	1	1	0	0	-1	5	1	0.00000	1.00000	-6.71225E-010	2.97239E-013

7. Add in two top mirrors and optimize.
 - Remove variables on bottom mirrors and only optimize Z-Position of the two top mirrors.
 - Use 45° for Y-Tilt only.
 - Manually adjust by X & Y Positions of mirrors to fit in into clear apertures of surfaces created in step 3.
 - In merit function, include segment optimization of ray leaving parabolic mirror to top right mirror, and include the last ray propagation's segment.

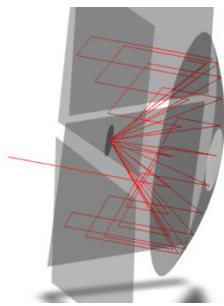


Object Type	Comment	X Position	Y Position	Z Position	Tilt About X	Tilt About Y	Tilt About Z	Material	Radius	Conic	Maximur
Source Ray	Alignment Ray	-31.00000	0.00000	-60.00000	0.00000	0.00000	0.00000	-	1	0	1.00
Standard Surface	Parabolic Mirror	0.00000	0.00000	0.00000	0.00000	0.00000	0.00000	MIRROR	-70.00000	-1.00000	39.00
Standard Surface	Thin Disk Mirror	0.00000	0.00000	-35.00000	0.00000	0.00000	0.00000	MIRROR	0.00000	0.00000	5.00
Rectangle	Mirror 1	22.00000	-21.50000	-33.00000	8.89098 V	-44.29887 V	9.00000	MIRROR	25.40000	25.40000	
Rectangle	Mirror 2	-13.50000	-29.00000	-33.49541 V	8.89098 P	44.29887	9.00000	MIRROR	25.40000	25.40000	
Rectangle	Mirror 3	22.90000	30.00000	-32.95000	0.00000	-45.00000	2.75000	MIRROR	25.40000	25.40000	
Rectangle	Mirror 4	-22.80000	30.25000	-33.05000	0.00000 P	45.00000	0.00000	MIRROR	25.40000	25.40000	
Standard Surface		-29.48275	9.57953	0.00000	0.00000	0.00000	0.00000		0.00000	0.00000	2.50
Standard Surface		-29.48275 P	-9.57953 P	0.00000	0.00000	0.00000	0.00000		0.00000	0.00000	2.50
Standard Surface		29.48275 P	9.57953 P	0.00000	0.00000	0.00000	0.00000		0.00000	0.00000	2.50
Standard Surface		29.48275 P	-9.57953 P	0.00000	0.00000	0.00000	0.00000		0.00000	0.00000	2.50
Standard Surface		9.57953 P	-29.48275 P	0.00000	0.00000	0.00000	0.00000		0.00000	0.00000	2.50
Standard Surface		-9.57953 P	-29.48275 P	0.00000	0.00000	0.00000	0.00000		0.00000	0.00000	2.50
Standard Surface		9.57953 P	29.48275 P	0.00000	0.00000	0.00000	0.00000		0.00000	0.00000	2.50
Standard Surface		-9.57953 P	29.48275 P	0.00000	0.00000	0.00000	0.00000		0.00000	0.00000	2.50

Type	Surf	Src#	Splt?	Pol?	Seg#	Data	Source #	Target	Weight	Value	% Contrib
NSRA	1	1	0	0	6	4	1	-1.00000	0.00000	-0.98769	0.00000
NSRA	1	1	0	0	6	1	1	-29.48275	0.00000	-29.48275	0.00000
NSRA	1	1	0	0	6	2	1	-9.57953	0.00000	-9.57953	0.00000
NSRA	1	1	0	0	7	4	1	0.00000	0.00000	2.30838E-012	0.00000
NSRA	1	1	0	0	7	5	1	0.00000	0.00000	3.65569E-013	0.00000
NSRA	1	1	0	0	-1	1	1	0.00000	1.00000	-1.23060E-006	50.06252
NSRA	1	1	0	0	-1	2	1	31.00000	1.00000	31.00000	49.93748
NSRA	1	1	0	0	-1	4	1	0.00000	1.00000	-7.47291E-012	1.84612E-009
NSRA	1	1	0	0	-1	5	1	0.00000	1.00000	-6.72851E-012	1.49664E-009

8. Once mirrors are positioned ideally, delete surfaces from step 3, and add in the Thin Disk.

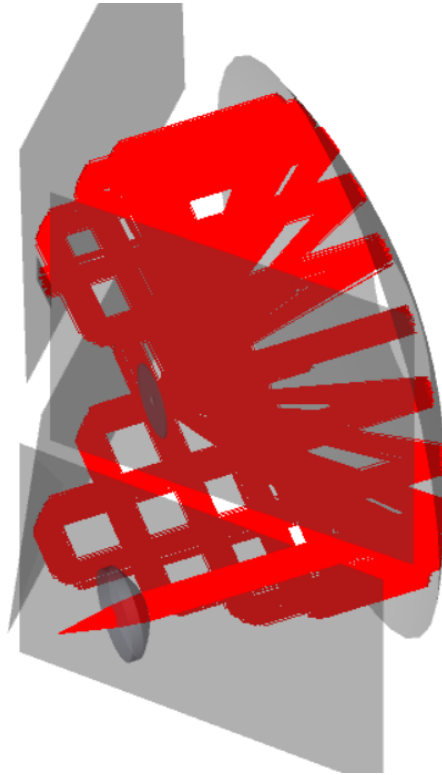
- Manually adjust Z Position of Thin Disk so beams overlap.
- Thin disks back face needs to reflect and front face needs to transmit.



Object Type	Comment	X Position	Y Position	Z Position	Tilt About X	Tilt About Y	Tilt About Z	Material	# Layout Rays	# Analysis Rays	Power(Watts)	Waver
Source Ray	Alignment Ray	-31.00000	0.00000	-60.00000	0.00000	0.00000	0.00000	-	1	0	1.00000	
Standard Surface	Parabolic Mirror	0.00000	0.00000	0.00000	0.00000	0.00000	0.00000	MIRROR	-70.00000	-1.00000	39.00000	10.00
Standard Lens	Thin Disc	0.00000	0.00000	-35.13549 V	0.00000	0.00000	0.00000	BPH35	0.00000	0.00000	5.00000	5.00
Rectangle	Mirror 1	22.00000	-21.50000	-33.00000	8.89098 V	-44.29887 V	9.00000	MIRROR	25.40000	25.40000		
Rectangle	Mirror 2	-13.50000	-29.00000	-33.49541 V	8.89098 P	44.29887	9.00000	MIRROR	25.40000	25.40000		
Rectangle	Mirror 3	22.90000	30.00000	-32.95000	0.00000	-45.00000	2.75000	MIRROR	25.40000	25.40000		
Rectangle	Mirror 4	-22.80000	30.25000	-33.05000	0.00000 P	45.00000	0.00000	MIRROR	25.40000	25.40000		

9. Use default merit function to optimize Z position of thin disk.
 - Add a detector face to be 0.00001mm in front of the HR side of the thin disk.
10. Add in source type into setup, and add in source collimation lens.
 - Use sequential analysis to determine optimal placement of collimation lens in relation to the source. Set the system up to be double telecentric with the parabolic mirror focal length the same as the designed system.
11. Use default merit function again to optimize Z position of Thin Disk.

Object Type	Comment	X Position	Y Position	Z Position	Tilt About X	Tilt About Y	Tilt About Z	Material	# Layout Rays	# Analysis Ra	Power(Watts)	Wavenumber	f
1 Source Radial *	DILAS 793nm Diode	-31.00000	0.00000	-60.00000	0.00000	0.00000	0.00000	-	100	10000000	1.00000	0	
2 Even Asphere Lens *	Thorlabs 1210-B Lens	-31.00000	0.00000	-52.38258	0.00000	0.00000	0.00000	S-LAH64	6.25063	4.25000			
3 Standard Surface *	Parabolic Mirror	0.00000	0.00000	0.00000	0.00000	0.00000	0.00000	MIRROR	-70.00000	-1.00000	39.00000	10.00000	
4 Standard Lens *	Thin Disc	0.00000	0.00000	-35.13549	0.00000	0.00000	0.00000	BPH35	0.00000	0.00000	5.00000	5.00000	
5 Detector Rectangle *	Thin Disc HR Surface	0.00000	0.00000	-34.88548	P	0.00000	0.00000		0.50000	0.50000	500	500	
6 Detector Rectangle *	Thin Disc HR Surface	0.00000	0.00000	-35.13548	P	0.00000	0.00000		0.50000	0.50000	500	500	
7 Rectangle *	Mirror 1	22.00000	-21.50000	-33.00000	8.89098	-44.29887	9.00000	MIRROR	25.40000	25.40000			
8 Rectangle *	Mirror 2	-13.50000	-29.00000	-33.49541	-8.89098	44.29887	P	9.00000	MIRROR	25.40000	25.40000		
9 Rectangle *	Mirror 3	22.90000	30.00000	-32.95000	0.00000	-45.00000	2.75000	MIRROR	25.40000	25.40000			
10 Rectangle *	Mirror 4	-22.80000	30.25000	-33.05000	0.00000	45.00000	P	0.00000	MIRROR	25.40000	25.40000		
11 Detector Rectangle *	End Absorber	0.00000	31.00000	-50.00000	0.00000	0.00000	0.00000		2.50000	2.50000	1	1	



Appendix C - Pump Chamber Alignment Procedure

Components Needed

>5" Collimator

Pinhole Alignment Cards

Thin Disk Reference Mirror

Camera and Monitor

The alignment is a very delicate process and takes time. Careful understanding of which components to adjust are absolutely critical since small detuning of alignment at later steps, especially the fold mirrors, will cause the system to not perform as required.

Procedure

1. Align collimator to table axis. In this case, the interferometer was used and has already been aligned to the table.
 - Ensure collimator has at least a 5" diameter exit beam and uses a focal length of 500mm or better. Accuracy is key for the 4 fold mirrors.
2. Layout table full of components and set approximate heights and locations on components to ensure everything fits properly. See Solidworks model for approximate reference locations. Once complete, move parabolic mirror out of the way.
 - This includes the thin disk pump optics including fold mirrors, parabola, thin disk alignment mirror, and reference flat.
 - Ensure translation stages are all set in the middle locations for maximum available adjustability later in process.
 - Ensure thin disk alignment mirror has z translation in fixture, then slide to closest focused spot of parabolic mirror with the physical X and Y location centered in the parabola through hole. This will not be known at this point so estimated guess is good enough.
3. Position the far field white retro-reflection card so that the outer beam hole is passing in between the bottom fold mirror and top fold mirror (as in the optical Zemax design).
 - On white retro-reflection card, ensure alignment holes are such that vertical holes are as vertical as possible. Right angle tools and rulers should be used to help, but are not mandatory.

- Ensure white retro-reflection card is extremely close to collimator and is perpendicular to optical axis. See figure 4.17.
4. Align both the thin disk reference mirror and the retro-reflection flat. Holes should be aligned such that it super imposes over far field retro-reflection holes.
 5. Align small white retro-reflection cards to top and side beams on the breadboard. The holes need to be very well centered, since this will be the reference for all later alignments.
 6. Remove fold mirrors from breadboard, and ensure parabola mechanical reference clips are loose on table. (If previously aligned, do not loosen.)
 - The clips will provide a rough alignment when added back into the system later in the process.
 - Ensure retro-reflection flat and thin disk alignment mirror are still aligned.
 7. Spin breadboard table around so the thin disk alignment mirror faces opposite of the collimator and align the retro-reflection flat to the collimator by only using the breadboard table screws.
 - Ensure beams go through small white retro-reflection cards placed down in step 5.
 - Do not adjust reference flat screws! Only breadboard table screws.
 8. Add in parabolic mirror and align it so the beam is focused onto thin disk alignment mirror by using the white retro-reflection beams seen on white retro-reflection card.
 - Do not adjust the tip-tilt on thin disk reference mirror. Be gentle when adjusting z-translation so as not to move the tip-tilt alignment. Best to avoid touching z-translation on thin disk alignment mirror, but if parabolic mirror has ran out of travel, adjust Z on thin disk alignment mirror, but start process over at step 2.
 - See section 4.3.1 and figure 4.19 for alignment process and beam patterns on white retro-reflection card.
 - Once aligned,
 - i. Tighten down parabolic mechanical reference clips.
 - ii. Remove parabolic mirror temporarily.
 - iii. Add back in parabolic mirror, and press into mechanical references.

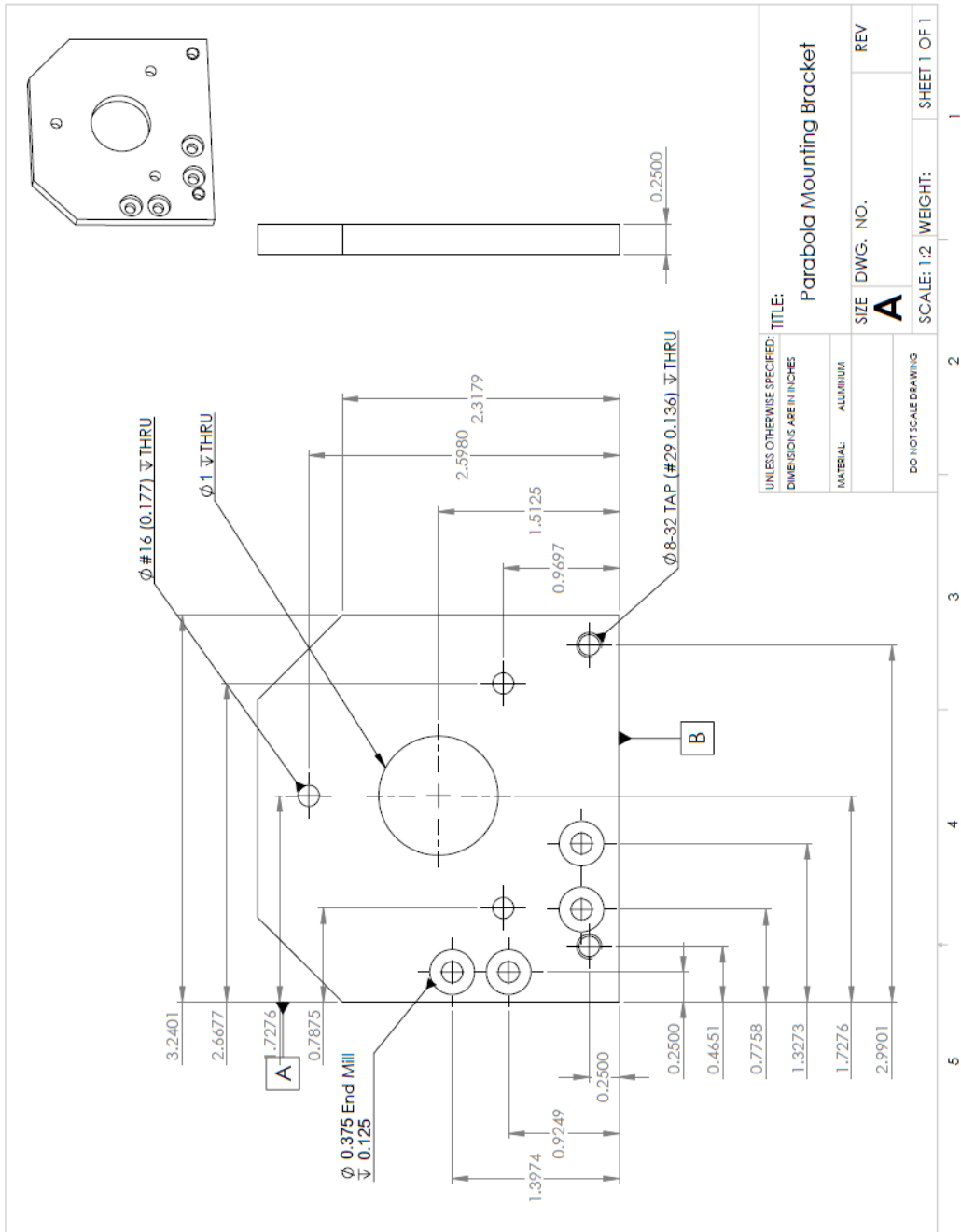
- iv. Tighten down parabolic mirror and ensure retro-reflection spots are still aligned. If not, repeat step 8.
9. Spin breadboard around and align the retro-reflection flat to the collimator using the breadboard adjusters and center beams with the small white retro-reflection cards.
 - Do not adjust the thin disk reference mirror. Both thin disk reference mirror and retro-reflection flat should still be aligned.
 - If the retro-reflection reference is off from the thin disk alignment mirror; something was knocked out of place. You must start over at step 4.
10. Add in two bottom flat mirrors to setup and align to white retro-reflection holes. See section 4.3.2 and figures 4.20 and 4.21.
 - Using the second near field white retro-reflection card helps alignment go quicker.
 - Ensure mirrors are clean before placing in setup.
 - Ensure to align to proper alignment holes for design.
 - Ensure beam placement is within clear aperture of mirrors.
 - Tricks to start are,
 - i. Approximately align mirror bottom left mirror so post reflection beam is bending the beam 90° to optical axis and so mirror fits within clear aperture of other beams in design.
 - ii. Add in bottom right mirror to setup and adjust rotational angle (in 1" mirror mount) on bottom right mirror to match bottom left mirror. See Solidworks angles/rotations of four fold mirrors.
 - iii. Position and tip-tilt bottom right mirror roughly so beams match to proper holes through white retro-reflection holes and so it is centered in clear aperture.
 - iv. Adjust positions and tip-tilt until for both mirrors until they are aligned to proper holes through white retro-reflection card and have beams centered in clear aperture.
**Trick is to align opposite mirror's beam spots over white retro-reflection cards holes by adjusting opposite mirror's adjusters.
 - v. Repeat d until all are aligned.

11. Place parabola on breadboard and ensure there is enough clearance for optics. Do not tighten or adjust parabola. Remove parabola when complete.
12. Add in two top fold mirrors to setup and repeat step 10 for top fold mirrors.
 - Ensure placement matches design in Solidworks and Zemax Models.
13. Double check alignment on all optics by ensuring alignment on all optics is reflected through correct holes on far-field white retro reflection card and that the small white retro-reflection cards are centered to correct beams.
 - They should all still be aligned. Minor changes may have occurred due to weight added onto breadboard.
 - If alignment is off for retro-reflection flat or thin disk reference mirror, you must restart at step 4.
14. Add in fiber mount and center hole with entrance beam from white retro-reflector card.
15. Add in parabolic mirror and gently press into mechanical reference mounts, then tighten down.
 - Be extremely careful.
 - Do not touch the translation or tip-tilt adjustments on any optics.
16. Once placed in and all screws are tightened down, move entire setup to room where laser can be turned on (and so collimation optics can be aligned).
 - At this point, the fold mirrors and parabola must not be changed. Doing so will throw the system out of alignment and make it very difficult to retain original characteristics.
 - Thin disk alignment mirror can be removed and replaced with thin disk setup, but not before collimation optics are aligned.
17. Set thin disk breadboard down onto table in new location and focus a camera onto the surface of the thin disk reference mirror.
18. Add in fiber laser into the fiber mount and adjust fiber mount so beam is coming in on axis to parabola and is centered through the small white

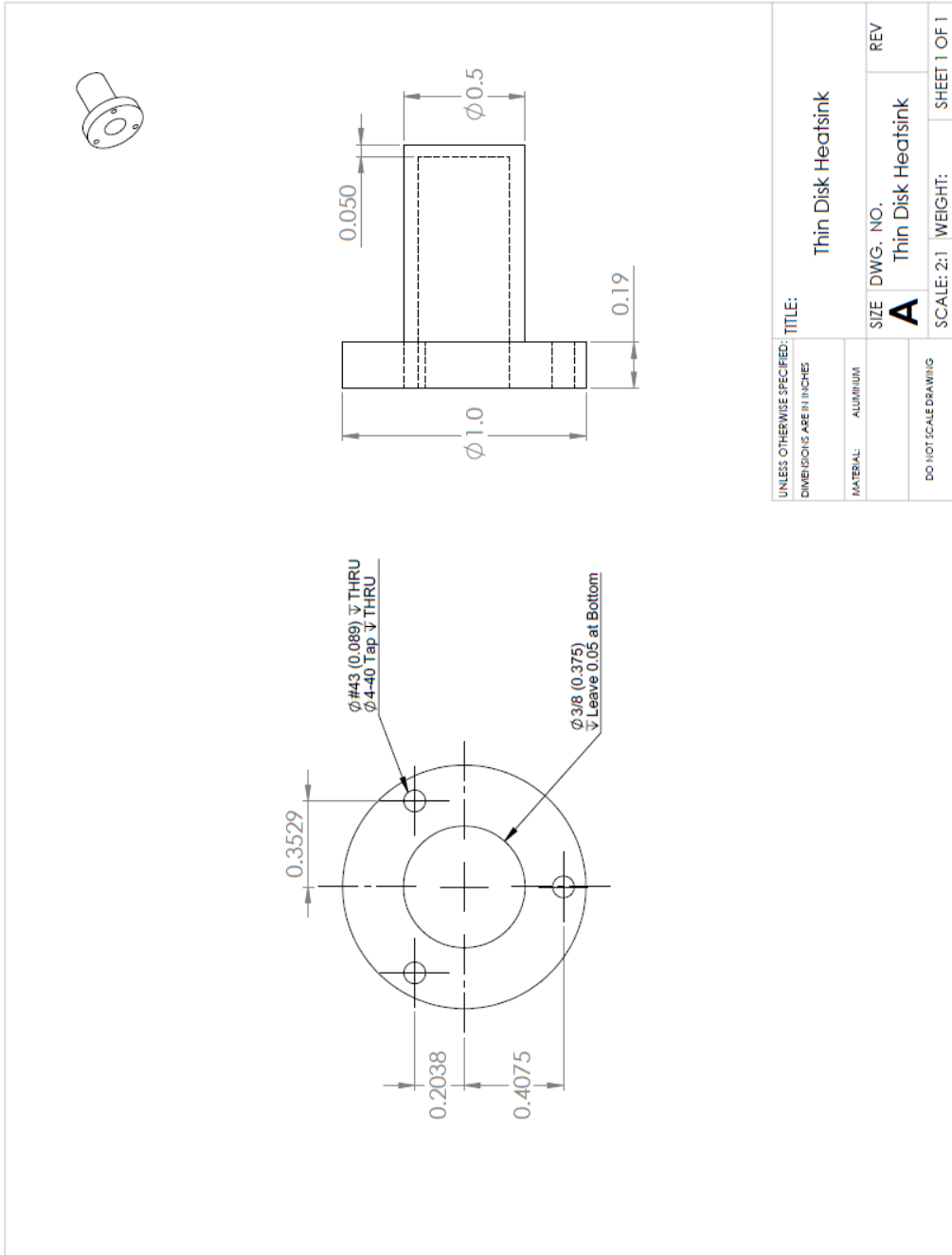
alignment card. Ensure camera is focused on thin disk. There should be faint clear speckle from laser on disk if camera is focused on surface.

19. Add in collimating optic and set focus using the camera. Collimated beam should go through center hole of small white card. You may need to move the fiber mount to center the beam through the hole. See section 4.3.3 and figures 4.22/4.24.
 - Set tip/tilt of collimating optics so back reflection is close to source.
 - **ONLY** adjust XYZ translation on collimating optic, and only Focus of Parabolic mirror. **DO NOT ADJUST ANY OTHER OPTICS!!**
20. Double check that all folding beams are in the clear apertures of the fold mirrors. Check that all spots are indeed overlapping.
21. Remove the camera and align HeNe beam over the thin disk pump spots and so HeNe beam is retro-reflected back to source. This sets the tip-tilt angle for later reference for the thin disk.
22. Remove thin disk reference mirror and add in actual thin disk and heatsink.
 - Do not adjust parabola or collimation optics.
 - Adjust tip-tilt on thin disk so HeNe beam is retro-reflected (from step 21).
 - Adjust focus of beams by using only the thin disk Z-translation.
 - Minor adjustments to the collimation optics can be made. Note; beams will not look round. That's ok.
23. Double check that spots on fold mirrors are centered in clear apertures and ensure all spots overlap on thin disk.
24. Pump Chamber is officially aligned, all that remains is standard resonator alignment not described.

Parabolic Mirror Mounting Bracket

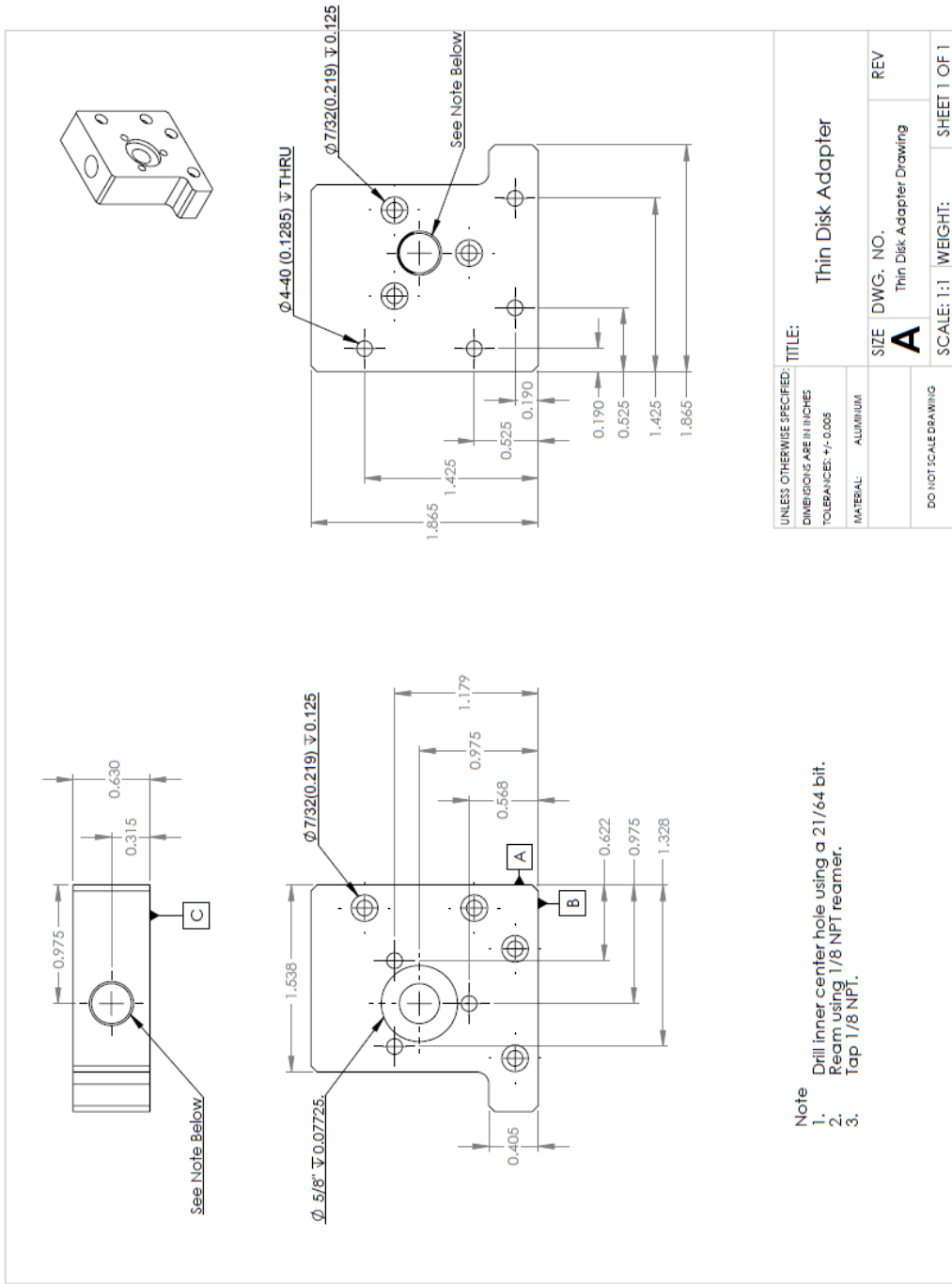


Thin Disk Heatsink



UNLESS OTHERWISE SPECIFIED: DIMENSIONS ARE IN INCHES		TITLE: Thin Disk Heatsink	
MATERIAL: ALUMINUM	SIZE A	DWG. NO. Thin Disk Heatsink	REV
DO NOT SCALE DRAWING		SCALE: 2:1	WEIGHT: SHEET 1 OF 1

Thin Disk Water Adapter



References

- [1] A. Killi, I. Zawishcha, D. Sutter, J. Kleinbauer, S. Schad, J. Neuhaus and C. Schmitz, "Current status and development trends of disk laser technology," *Solid State Lasers XVII: Technology and Devices*, vol. Proceedings of SPIE 6871, no. 68710L, 2008.
- [2] K. Scholle, S. Lamrini, P. Koopmann and P. Fuhrberg, "2 μm Laser Sources and Their Possible Applications," *Frontiers in Guided Wave Optics and Optoelectronics*, 2010.
- [3] Y. Kalisky, *The Physics and Engineering of Solid State Lasers*, Bellingham: SPIE, 2005, pp. 149-153.
- [4] A. Siegman, *Lasers*, Palo Alto, CA: University Science Books, 1986, p. 66.
- [5] W. Koechner, *Solid-State Laser Engineering*, vol. 6th, New York, NY: Springer Science+Business Media, Inc., 2006, pp. 81, 94-101, 219-225, 282, 458-473.
- [6] M. Javadi-Dashcasan and F. Hajiesmaeilbaigi, "Optimizing the Yb:YAG thin disc laser design parameters," *Optics Communications*, vol. 281, no. 18, pp. 4753-4757, 2008.
- [7] A. Giesen, A. Voss, K. Wittig, U. Brauch and H. Opeower, "Scalable concept for diode-pumped high-power solid-state lasers," *Applied Physics B*, vol. 58, no. 5, pp. 365-372, May 1994.
- [8] A. Giesen, "Results and scaling laws of thin-disk lasers," *Solid State Lasers XIII: Technology and Devices*, 8 July 2004.

- [9] A. Tyler, E. Korczynski and K. Sumantri, "Diode-Pumped Solid-State Lasers: Edge pumping drives slab-laser performance," 03 01 2000. [Online]. Available: <http://www.laserfocusworld.com/articles/print/volume-36/issue-3/features/diode-pumped-solid-state-lasers-edge-pumping-drives-slab-laser-performance.html>.
- [10] R. Xu, L. Xu, L. Hu and J. Zhang, "Structural Origin and Laser Performance of Thulium-Doped Germanate Glasses," *J. Phys. Chem. A*, vol. 115, no. 49, pp. 14163-14167, 15 November 2011.
- [11] L. Esterowitz, "Diode Pumped Holmium, Thulium And Erbium Lasers Between 2 and 3um Operating CW At Room Temperature," 1989.
- [12] X. Zhu, *Measured data of Thulium³⁺ Germanate Absorption and Emission Cross Section Data*.
- [13] R. Paschotta, "Doping Concentration," RP Photonics Consulting GmbH, [Online]. Available: https://www.rp-photonics.com/doping_concentration.html.
- [14] K. Contag, M. Karszewski, C. Stewen, A. Giesen and H. Hugel, "Theoretical modelling and experimental investigations of the diode-pumped thin-disk Yb:YAG laser," *Quantum Electronics*, vol. 29, no. 8, pp. 697-703, 1999.
- [15] A. Giesen and J. Speiser, "Fifteen Years of Work on Thin-Disk Lasers: Results and Scaling Laws," *IEEE journal of Selected Topics in Quantum Electronics*, vol. 13, no. 3, May 2007.
- [16] J. Zuclich, D. Lund and B. Stuck, "Wavelength dependenc of ocular damage thresholds in the near-IR to far-IR tansion region: proposed revisions to MPEs," *Health Physics*, vol. 92, January 2007.

- [17] G. M. Hale and M. R. Querry, "Optical constants of water in the 200nm to 200um wavelength region," *Appl. Opt.*, vol. 12, pp. 555-563, 1973.
- [18] J. Dong, M. Bass, Y. Mao, P. Deng and F. Gan, "Dependence of the Yb³⁺ emission cross section and lifetime on temperature and concentration in yttrium aluminum garnet," *Journal of the Optical Society of America B*, vol. 20, no. 9, pp. 1975-1979, 2003.
- [19] Q. Liu, X. Fu, M. Gong and L. Huang, "Effects of the temperature dependence of absorption coefficients in edge-pumped Yb:YAG slab lasers," *Journal of the Optical Society of America B*, vol. 24, no. 9, pp. 2081-2089, 2007.
- [20] J. E. Shelby, "Viscosity and Thermal Expansion of Alkali Germanate Glasses," *Journal of the American Ceramic Society*, vol. 57, no. 10, pp. 436-439, October 1974.
- [21] H. Weber and N. Hodgson, *Laser Resonators and Beam Propagation*, vol. 2nd, New York, NY: Springer Science+Business Media, Inc, 2005, pp. 261-264.
- [22] D. Vukobratovich and S. Vukobratovich, *Introduction to Opto-Mechanical Design*, Tucson: Society of Photo Optical, 1993, p. 249.
- [23] S. Vatik, I. Vedin, M. Segura and X. Mateos, "Efficient thin-disk Tm-laser operation based on Tm:KLu(WO₄)₂/KLu(WO₄)₂ epitaxies," *Optics Letters*, vol. 37, no. 3, pp. 356-358, 2012.
- [24] J. Wu, Z. Yao, J. Zong and S. Jiang, "Highly efficient high-power thulium-doped germanate glass fiber laser," *Optics Letters*, vol. 32, no. 6, pp. 638-640, 2007.

- [25] Q. Fang, W. Shi, K. Kieu, E. Petersen, A. Chavez-Pirson and N. Peyghambarian, "High power and high energy monolithic single frequency 2um nanosecond pulsed fiber laser by using large core Tm-doped germanate fibers: experiment and modeling," *Optics Express*, vol. 20, no. 15, pp. 16410-16420, 2012.
- [26] M. Najafi and A. Sepehr, "Simulation of thin disk laser pumping process for temperature dependent Yb:YAG property," *Optics Communications*, vol. 282, no. 20, pp. 4103-4108, 15 October 2009.
- [27] E. Bastow, "Indium-Copper Intermetallics in Soldering," 13 January 2012. [Online]. Available: <http://www.indium.com/blog/indium-copper-intermetallics-in-soldering.php>.